OSTEOGENIC DIFFERENTIATION IN PREOSTEOBLAST MC3T3-E1 CELLS INDUCED BY BETA TRICALCIUM PHOSPHATE BIOGLASS COMPOSITE.

by

CHIEN-NING YAO

THESIS

Presented to the Faculty of the Graduate School of

The University of Texas at Arlington in Partial Fulfillment

of the Requirements

for the Degree of

MASTER OF SCIENCE IN MATERIALS SCIENCE AND ENGINEERING

THE UNIVERSITY OF TEXAS AT ARLINGTON

JULY 2016

ACKNOWLEDGEMENTS

I never think that this part will be the most difficult part for me to go with. No word can explain how lucky I feel I am....

My deepest gratitude goes first and foremost to Professor Aswath, my supervisor, for his constant encouragement and guidance. He is very busy, but he still spares a lot of time for solving my problems and then keep busier for his remaining time. He never blames me, but always let me know I need to be more and more self-motivated. I will never forget how nice and helpful he is, and he is always the most influential teacher in my life.

Second, I would like to express my heartfelt gratitude to Professor Varanasi, who led me into the world of being critical thinking and knowledgeable. He always can give me very helpful suggestion and let me know the direction of my experiments and even my life. He has a very soft heart but he never let you know.

I am also greatly indebted to Dr.Shiakolas and Dr. Yaowu Hao at the Department of mechanical Engineering and material science engineering, who have instructed and helped me a lot in the past two years.

Then I cannot express how lucky am I that I can meet Dr. Felipe Monte, he is a doctor but he never gets on his high horse. I feel so respected treated whenever I worked with him. He is really a strong backup of mine, and I will always think about him when I meet any situation and he always can solve the problem for me. Moreover, my labmate, David, thank for his kindness and doing so much analysis for me and let me can do the other work in different place. It's truly my pleasure to work with so much great people in Dr. Aswath's lab. Ami, Tugba,Vinay,Vibhu and Prashanth Ravi, Phillip Zachary James in Dr.Shiakolas's lab

And my parents, who always support me and respect my decision. I will never let them down but let them always be the happiest parents.

I feel truly grateful to thank everyone who helps me for these two years, these 25 years. Without you, I won't be here.

July 24, 2016

ABSTRACT

OSTEOGENIC DIFFERENTIATION IN PREOSTEOBLAST MC3T3-E1 CELLS INDUCED BY CALCIUM PHOSPHATE BIOGLASS COMPOSITE

CHIEN-NING YAO, MS

The University of Texas at Arlington, 2016

Supervising Professor: Pranesh Aswath

The use of bioactive material from bioceramic and composite components to support bone cell and tissue growth is an interesting area of medical field. Calcium phosphate ceramics are biocompatible and may develop interactions with human living bone tissues. Bioactive calcium phosphates, beta -tricalcium phosphate (β-TCP), have been intensively investigated as the cell scaffold for bone tissue engineering because it is well recognized that they are compatible to natural bone tissue and osteoconductive. In this research we will discuss two types of biomaterial with different kind of composition—(a) a cement type and (b)a scaffold type of biomaterial that can be applied to different kind of bone effect treatment.

β-TCP is advantageous from the viewpoint of dissolution, but brittle compare to the other CPC. Its brittleness posses a limitation of their common clinical use. Current challenges include the engineering of materials that can match both the mechanical and biological property to enhance the recovery of bone failure.

For the study, bioactive glass, gelatin, and laponite solution that are known for their bioactive properties will be used to create a bioactive scaffold with β-TCP. Groups of scaffold will be analysis in three approaches (1) Material characterization by using SEM, FTIR, XRD, EDS, goniometric machine…etc (2) In Vitro Study with cell culture, MTS assay, cell adhesion, raman spectra….etc (3) Development of Three Dimensional Printed Scaffold. Findings suggest that the optimum composition of b-TCP with 30% bioglass and either 2wt% laponite or 2wt% Gelatin can lead to higher mechanical property and enhanced formation of hydroxyapatite(HA). Cellular differentiation studies with xxxx cells in the presence of ascorbic acid (50 mg/L) also demonstrated improved collagen fiber bundles formation compared to other compositions and the control coverslip. These results support the larger concept that beta tri-calcium phosphate with Bioglass and binder like gelatin and laponite could control bone formation by inducing the osteogenic differentiation.

With the understanding of the material characterization and pathology environment, using specialized three-dimensional (3D) printing technology we created a porous structure to promote bone repair.

Table of Content

List of Illustrations

List of Table

Chapter 1

Introduction

According to the statistics, approximately half of the population happened at least one bone fracture during their lifetime[1] In this case, surgery might be necessary. The more research had been put on minimize the invasive techniques and trying to offer special benefits for patients such as fewer surgery operation, shorter recovery time and less pain even less time staying in medical service. Therefore, potential bone grafts application can reduce the risk of invasive surgery . Such formulations are known as self-setting formulations. They possess an ability to solidify in the appropriate period, giving strength to the implantation sites.

Calcium phosphate (CaP) compound are increasing attention and importance in the field of biomaterial and bone substitutes [2]. The difference in the composition and structure of CaP compound have great profound effect no matter in vitro or in vivo study. Therefore, the main goal of this research will focus on the bone repair

material, beta- tricalcium phosphate, provide a simple, but comprehensive presentation of this CaP compounds.

Beta- tricalcium phosphate is an advantageous powder from the viewpoint of biodegradability, but brittle and lower mechanical property and injectability. By combining with some binder materials, such as gelatin and laponite. It has been reported that the combination improves the degradation and mechanical properties for scaffolds[3]–[5] has also been trial to overcome the drawback of material properties.[6]

The optimal scaffold for bone repair should be able to adjust to the damaged bone area, prevent infection, provide mechanical stability, recruit cells to the site for repair, promote faster growing of bone, and eventually remodel leaving normal bone behind. Using specialized three-dimensional (3D) printing technology we can design custom scaffolds for bone repair composed of materials with these optimal characteristics and even combine them with some growth factor that can provide improved healing of certain bone area. beta- tricalcium phosphate will also be modified to a porous three dimensional scaffold.

1.1 Motivation for the Research

For a better technique and shorter recover time to heal the bone injury, types of bioactive scaffold/cement were created. Not so much information about all the combination of detail material characterization of beta tricalcium phosphate combined with different proportion of Bioglass 45S5 with laponite and gelatin solution was provided, so the suitable scaffold / material exhibiting adequate mechanical and biological properties were provided to enable tissue regeneration by exploiting the body's inherent repair mechanisms, like bone healing and bone remodeling. Biodegradability and bioactivity are to be combined in an optimized tissue engineering scaffold, then the design of this composite materials offers an exceptional opportunity: Composites allow for the creation of bioresorbable and bioactive scaffolds with tailored physical and mechanical properties. For more application, porous scaffold would be designed for customized shape and structure for different kinds of fracture. Biological interactions in vitro can be the basic idea of complex multiple interaction when it applied to real pathology. In this case, the study of a well

defined system in vitro study may serve as an approximation to understanding biological behavior after the analysis of the material characterization.

1.2 Objectives of the Research

Broadly defined, the goal of this study is to improve the general understanding of the beta tri-calcium phosphate cement or scaffold when it combines with Bioglass and different kind of mixing solution like Na_2HPO_4, gelatin and laponite. By applying a materials science and engineering-based approach to (a) Better mechanical property (b) enhance rapid bone differentiation with respect to both healthy bone and diseased bone chemistry, and (c) future expectation of developing methods to create a porous three dimensional scaffold for the need of customize shape of scaffold. Begin with improving these goal, it is important to first understand the initially formed diseased bone and the material feature even the chemistry at the ultrastructure level. In order to make comparison between groups of scaffold, the material will be identified at first. Simultaneously, groups of scaffold will be applied to in vitro study to detect the chemistry to mimic the real pathology.

After analysis of the material characterization and in vitro model, the third aim of this study is to optimized a cement to apply to three dimensional printing research.

1.3 Structure of the Research

This thesis research is composed of seven chapters.

Chapter 1 introduces the basic motivation for this study and provides some context.

Chapter 2 will introduce some background including the bone structure and some process when the fracture occurred and how the bioactive ceramic/glass acting to help healing.

Chapter 3 gives an overview of the experimental procedures and technique related to this research and a background principle of methods.

Chapter 4 discusses the Characterization and Design of Tricalcium Phosphate Based Scaffolds for two aspects: material and biological analysis. All the information and detail method will be illustrated in this chapter.

After the overall study of the material characterization, the three dimensional structure will be introduced in chapter 5 for a basic setting of extruding material with a lab created printing machine.

Chapter 6 will be the possible application of the bioactive scaffold related to some medical field and discuss the whole part of this experiment and concluded.

Chapter 2

Background

In early 1980s, researchers discovered self setting calcium orthophosphate cements[2] which are bioactive and biodegradable bioceramic in the form of a powder and a liquid. With mixing, the paste was form and set and harden forming or a non-stoichiometric calcium deficient hydroxyapatite[7]. Either is remarkably biocompatible, and osteoconductive. Currently such formulations are widely used as synthetic bone grafts, but there are some disadvantages, such as weak mechanical property and low injectability. Beta tri-calcium phosphate (β-TCP) will be used in this research since it stays relatively stable in the body environment and it does not dissolve in body fluids at physiological pH level. Moreover, β-TCP has capability to establish chemical bonds with the hard tissues, fast setting time, excellent mouldability, outstanding biocompatibility[8].

Bioactive glasses are the first material that exhibits bioactive behavior[9]. These types of bioceramic are therefore rarely used in load-bearing tissue applications. An example of this type of bioceramic would be certain dissolvable silica-based bioglass 4S5S. With combine of the β-TCP and bioglass 4S5S, can provide more durable and bioactive bioceramic.

When defect of bone happens, more concern associated to bear load will be placed on different types of bone defect. Bone is a dynamic and highly vascularized tissue that continues to remodel throughout the lifetime of an individual. It plays an integral role in locomotion, ensures the skeleton has adequate load-bearing capacity. Creating a force endurable scaffold and help to recover bone defect is necessary to include in our aim.

2.1 The Structure of Bone

Bones can provide support, movement and protection in every occasion. Moreover, they also store calcium and phosphate and blood cells are formed in the marrow. Bones also play an important role in energy metabolism such as osteoblasts can secrete a hormone called osteocalcin which is what triggers the pancreas to secrete insulin. There is one-third of the bone structure are made of

organic compound just like some bone related cells, collagen fibers and matrix and the remaining part are the inorganic; some mineral salts such as calcium phosphate which make the bone hard and what preserve it long after the animal dies.

There are some hierarchy of formation associated to bone cell, osteoblasts, osteocytes and Osteoclast. Osteogenic cells are kinds of stem cells that can help form osteoblasts. Osteoblast are cells with single nuclei that synthesize bone. However, the group of organized osteoblasts together with the bone made by a unit of cells is usually called the osteon. Fig2.1

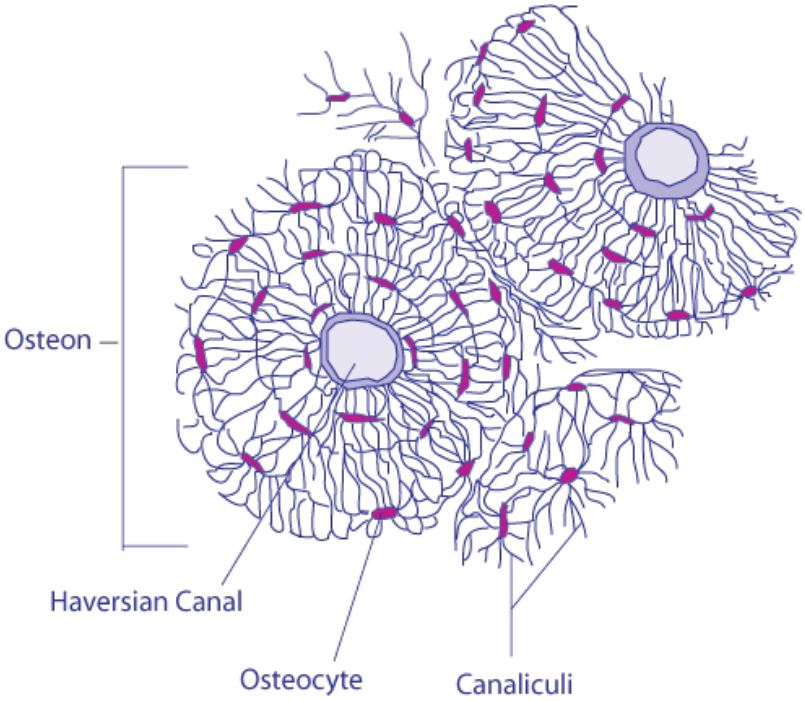

Fig 2.1 A group of organized osteoblasts together with the bone made by a unit of osteon cells. [10]

Osteoblasts lay out a lot of bone matrix called osteoid before the organic matrix is mineralized. Osteoblasts that are buried in matrix are called osteocytes and don't produce matrix anymore but simply maintain it.

Osteoclast comes from white blood cells. They have multiple nuclei and secrete HCl acid to break down mineral salts and secrete lysosomes. Basically, everything needs to break down organic parts of bone. It's totally normal to constantly break down and rebuild bone in response to stress or impact, and this is called **bone remodeling**.

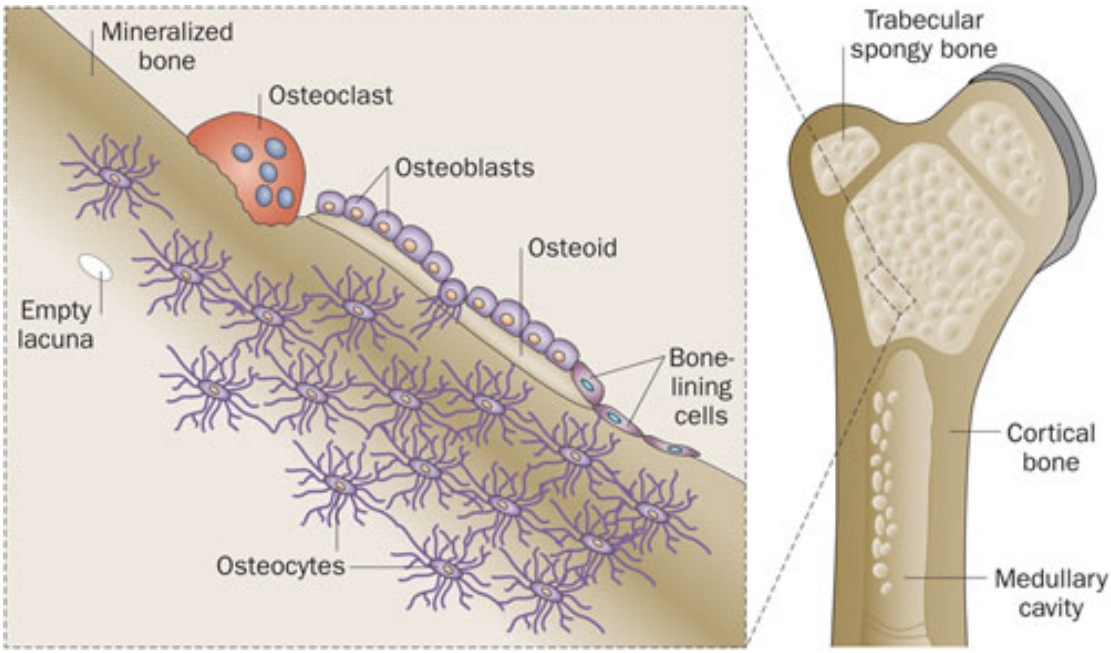

Fig 2.2 Microstructure and macrostructure of mammalian bone: osteoblasts, osteocytes and Osteoclast[11]

2.2 Bone Mineralization and Remodeling

There was some misunderstanding between bone growing and remodeling. Growing bone is just bone with a higher deposition to resorption rate. Therefore, growth stops when a balance between resorption and new bone formation is achieved. "In contrast to the lengthening of bone, the thickness and strength of bone must continually be maintained by the body. That is, old bone must be replaced by new bone all the time. This is accomplished as bone is continually deposited by osteoblasts, while at the same time, it is continually being reabsorbed (broken down and digested by the body system) by osteoclasts and this process is called bone remodeling. Osteoblasts are found on the outer surfaces of the bones and in the bone cavities. A small amount of osteoblastic activity occurs continually in all living bones (on about 4% of all surfaces at any given time) so that at least some new bone is being formed constantly [10]. Normally, except in growing bones, the rates of bone deposition and absorption are equal to each other so that the total mass of bone

remains constant.

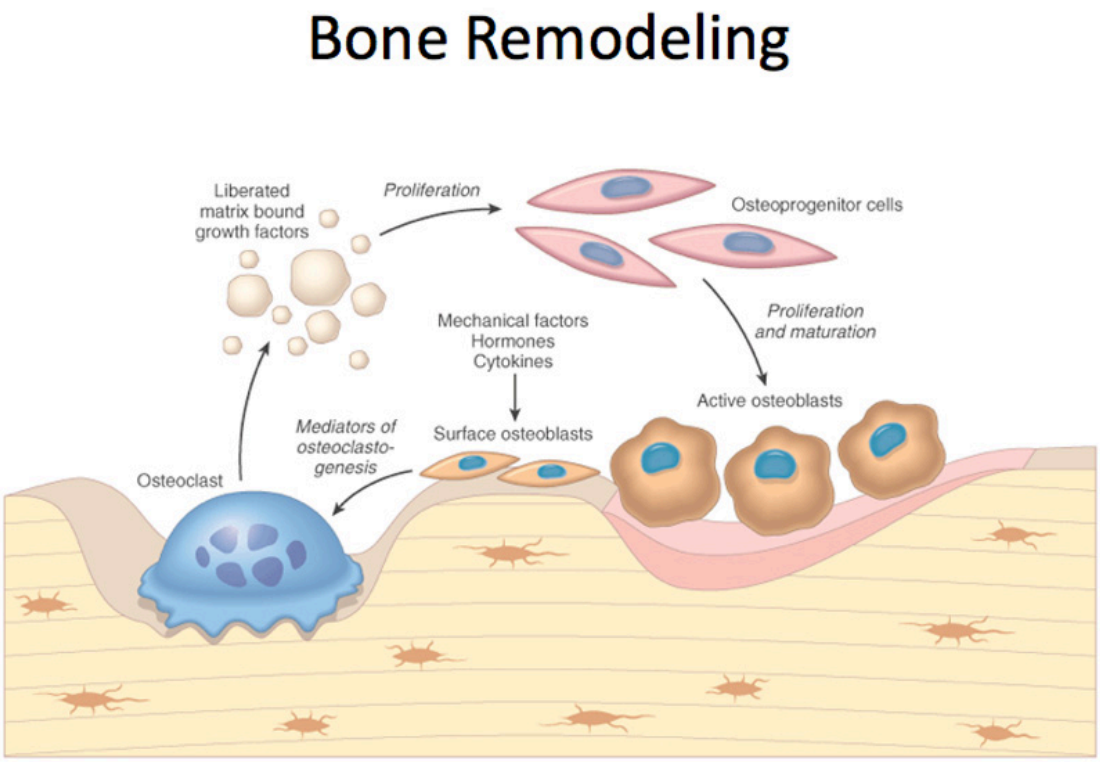

Fig.2.3 Bone remodeling process

The bone is a dynamic hard tissue that undergoes a continuous remodeling process to maintain skeletal strength and integrity, with 10% of the skeleton being replaced annually. In a finely balanced, coupled and sequential process (indicated by the dashed arrows), hematopoietic stem cell (HSC)-derived osteoclasts resorb bone which release growth factors and calcium and mesenchymal stem cell (MSC)-derived osteoblasts replace the voids with new bone, a process that is dependent on osteoblast

commitment, proliferation and differentiation coupled with osteoblast production of type I collagen and its subsequent mineralization to form the calcified matrix of bone. Osteocytes, which are terminally differentiated osteoblasts that are embedded in bone, sense mechanical strain, signal to osteoclasts and osteoblasts, and participate in the remodeling process[12]. Bone cells are osteoblast in origin and have been proposed to form both a canopy over remodeling sites and a layer over bone surfaces, as well as a conduit to communicate with osteocytes. The endosteum and periosteum (the lining on the inner and outer bone surfaces) contain a population of tissue macrophages, termed osteomacs, which are likely to have important roles in bone remodeling[12]. M-CSF, macrophage colony stimulating factor; RANK, receptor activator of NF-κB; RANKL, RANK ligand.

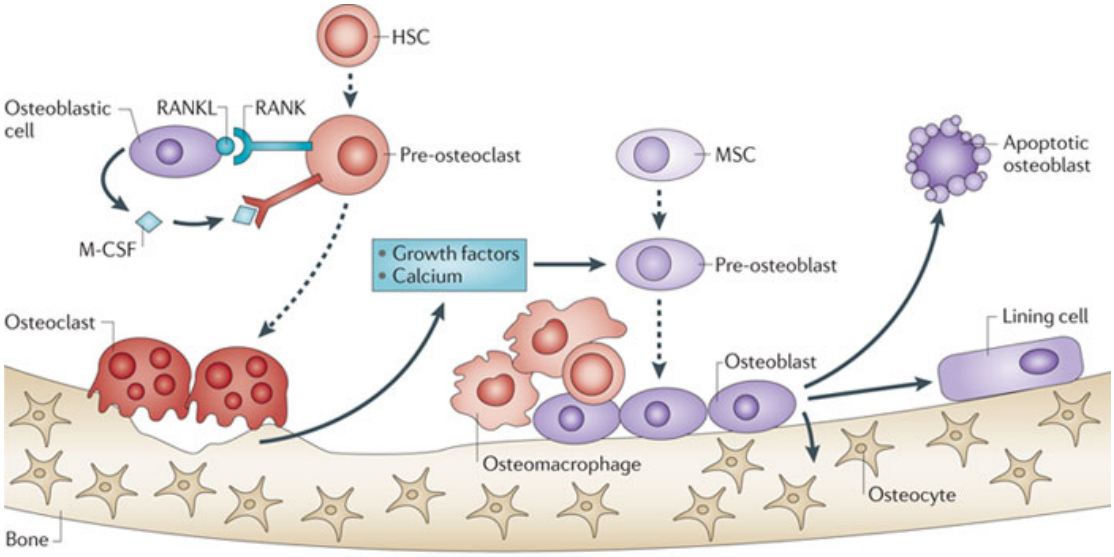

Fig2.4 Bone remodeling in molecular level process[12]

2.3 Biomaterials for Load-Bearing Applications in Bone

Biomaterials can enhance bone regeneration and increasing of potential clinical applications from the treatment of impact fractures to spinal fusion. The use of bioactive material scaffolds from bioceramic and polymer components to support bone cell and tissue growth is a longstanding area of interest[13]. Current challenges include creating the materials that can satisfy the mechanical property and the biological context of real bone tissue matrix and support the vascularization of large tissue constructs. Scaffolds with new levels of bio function that attempt to recreate nanoscale topographical and biofactor cues from the extracellular environment are emerging as interesting candidate biomimetic materials.

For load-bearing bone needs, neither polymers nor porous ceramics have the necessary compressive strength to replace cortical bone tissue. A few dense(>99.8%) hydroxyapatite and beta-tricalcium phosphate ceramic materials have been observed to meet the expectation to achieve the compressive strength of bone[14][15], however, these materials lack the necessary fracture toughness for therapeutic use in human loadbearing bone tissues[14].

Common approaches to reduce brittleness of the biomaterial cement (like tri-calcium phosphate and CPC cement) and to improve their mechanical performance for load-bearing applications include the modification of the cement liquid with polymeric additives such as collagen or gelatin[10][11], the addition of fibers to the cement matrix[17] or the use of dual-setting cements in which a dissolved monomer is simultaneously cross-linked during cement setting [18]. The most significant reinforcement strategies for calcium phosphate cements based on either intrinsic (porosity) or extrinsic (fiber addition, dual setting cement) material modifications which is shown in fig 2.5

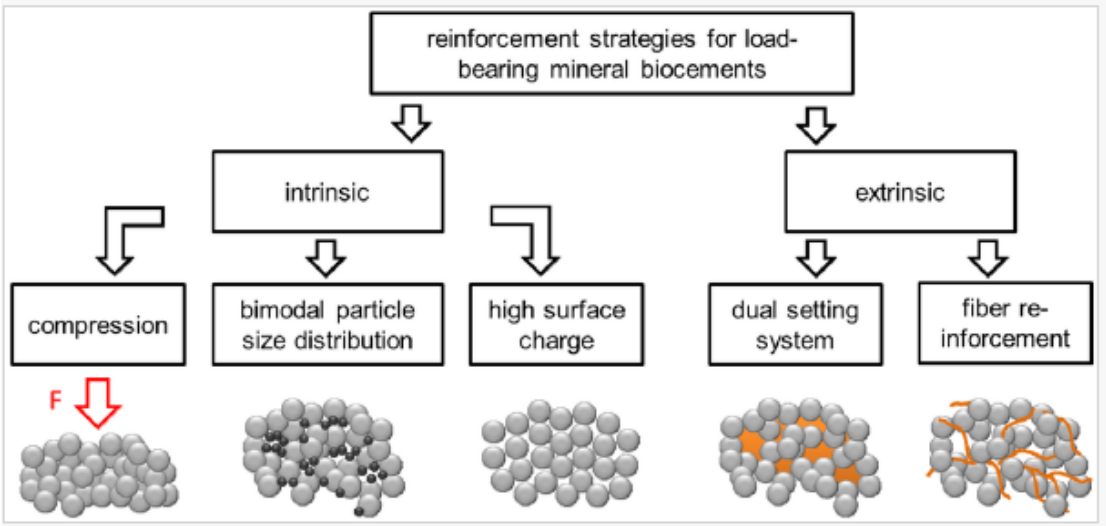

Fig.2.5 Strategies to reinforce mineral bio cement for load-bearing applications.[19]

In this research, we will improve the bioactive cement both from intrinsic and extrinsic part. Beta tri-calcium phosphate and bioactive glass has significant different particle size. In this case, ball milling process will improve the size distribution and make it becomes more amorphous and even lead to higher mechanical property.Fig 2.6. Large-sized particles(Bioglass) reinforced bioactive scaffold had much lower porosity density, on the other hand, higher relative density and superior mechanical properties comparing with the small-sized(β-TCP) particles reinforced scaffold and the mixture of bimodal grain size Fig 2.7/Fig 2.8 cement will lead to higher mechanical property. From extrinsic part, the binder like sodium hydro phosphate, gelatin, and laponite solution will be prepared as the dual setting system which benefit for even more significant increasing of mechanical property.

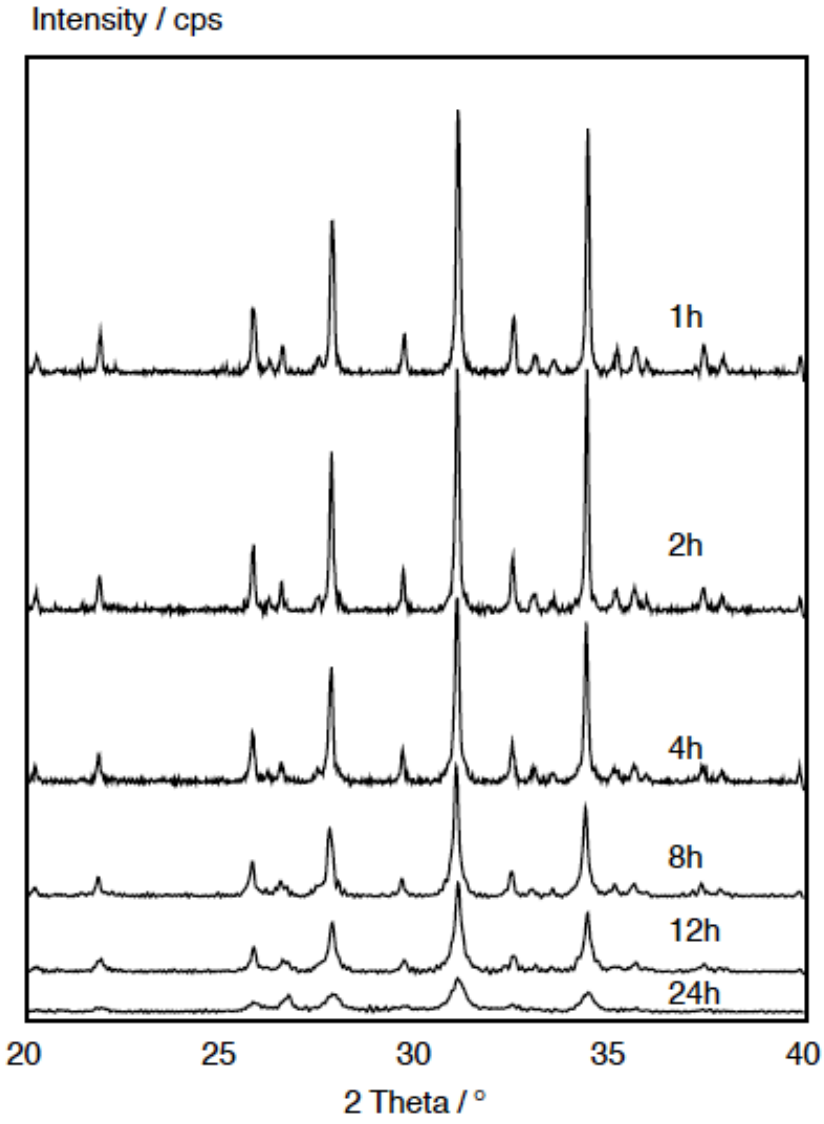

Fig 2.6 The X-ray pattern of β-TCP ball milling process with ethanol with different period of time[20].

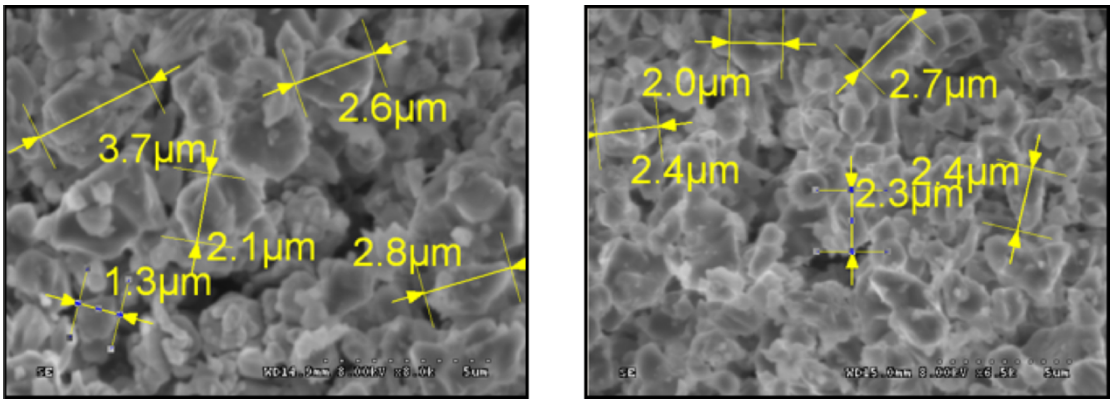

Fig 2.7 The average size of β-TCP is 2.43 μm measure by Hitachi S-3000N Variable Pressure SEM (STD value approximately equal to 0.62 μm)

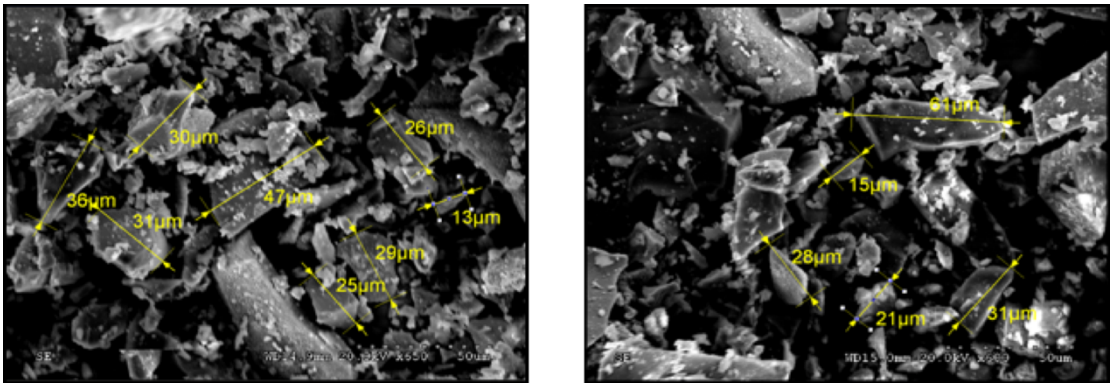

Fig 2.8 The average size of bioglass 4S5S after ball milling is 30.23 μm measure by Hitachi S-3000N Variable Pressure SEM (STD value approximately equal to 12.67 μm)

2.4 Bioactive Ceramics

Bioceramics is used for repairing and reconstructing the damaged parts of the muscular-skeletal system. The term “bioceramic”, may be bio-inert (alumina,

zirconia), resorbable (tricalcium phosphate), bioactive (hydroxyapatite, bioactive glasses, and glass-ceramics), or porous for tissue to growth (hydroxyapatite-coated metals, alumina). Applications include replacements for hips, knees, teeth and ligaments and repair for periodontal disease, reconstruction, and stabilization of the jaw bone, spinal fusion, and bone fillers after tumor surgery. Bioceramics are used in many types of medical procedures and are typically used as rigid materials in surgical implants and bioceramic materials also help to reduce wear and inflammatory response.

Table II. Types of Bioceramics –Tissue Attachment and Bioceramic Classification

Type of bioceramic	Type of attachment	Example
1	Dense, nonporous, nearly inert ceramics attach by bone growth into surface irregularities by cementing the device into the tissues, or by press fitting into a defect (termed morphological fixation).	Al_2O_3 (single crystal and polycrystalline)
2	For porous inert implants bone ingrowth occurs, which mechanically attaches the bone to the material (termed biological fixation).	Al_2O_3 (porous polycrystalline) Hydroxyapatite-coated porous metals
3	Dense, nonporous, surface-reactive ceramics, glasses, and glass-ceramics attach directly by chemical bonding with the bone (termed bioactive fixation).	Bioactive glasses Bioactive glass-ceramics Hydroxyapatite
4	Dense, nonporous (or porous), resorbable ceramics are designed to be slowly replaced by bone.	Calcium sulfate (plaster of Paris) Tricalcium phosphate Calcium phosphate salts

Table2-1 The types of bioceramics[21]

2.5 Bioactive Glasses

Glasses within a certain range of compositions in the SiO2-CaO-P_2O_5-Na_2O system were the first materials to exhibit bioactive behavior. Certain silica glass-ceramics also show bone bonding. Tlarge depth of focus by cohere are four classes of bioglass:

- 35-60 mol.% SiO_2, 10-50 mol.% CaO, 5-40 mol.% Na_2O: bioactive, bonds to bone, some formulations bond to soft tissues
- <35 mol.% SiO_2: non glass-forming
- >50 mol.% SiO_2, <10 mol.% CaO, <35 mol.% Na_2O: bioactive, resorption within 10–30 days
- >65 mol.% SiO_2: non-bioactive, nearly inert, gets encapsulated with fibrous tissue

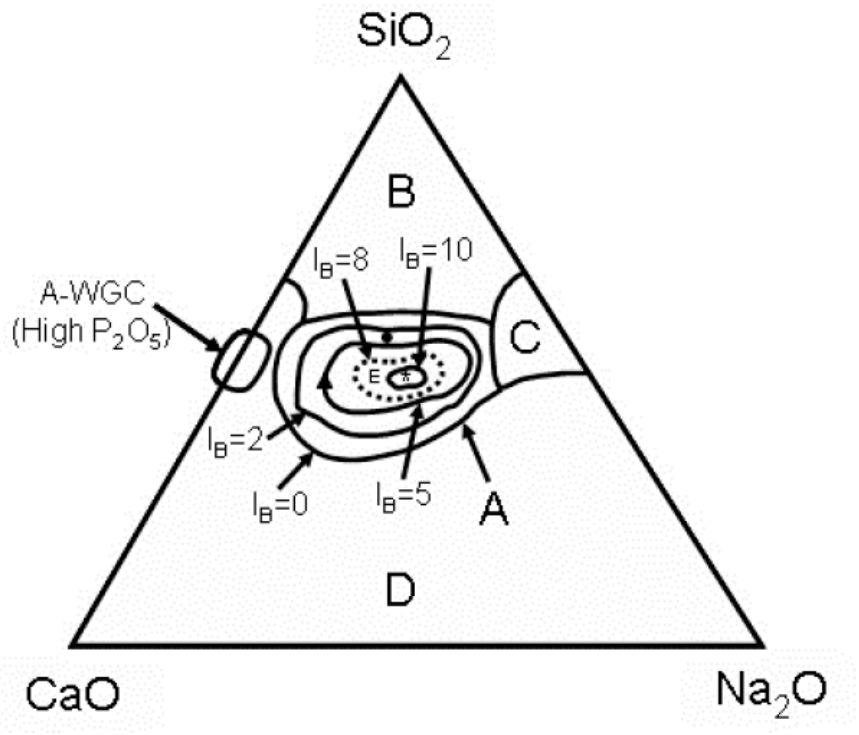

Fig 2.9 The class of bioglass, and the compositional of bioglass will lead to different bone bonding ability. All compositions in region A have a constant 6 wt. % of P_2O_5. Region E (soft tissue boding) is inside the dashed line where I_B>8 [* 45S5 Bioglass ®, ▲ Ceravital®, ●55S4.3 Bioglass ®, and the dot line (---) indicated to soft-tissue bonding ability ; I_B=100/t0.5bb, where t0.5bb is the time to have more than 50% of the implant surface bonded to the bone and I_B is bioactivity index[22].

The way result in bioactive glass bind to local bone is the reaction with the bioglass with ionic salts in physiological solution (blood plasma). Table 2.2 lists the concentration of inorganic salt species found in physiological solution.

Ion	Plasma (mM)
Na^+	142
K^+	5.0
Mg^{2+}	1.5
Ca^{2+}	2.5
Cl^-	103.0
HCO_3^-	27.0
HPO_4^{2-}	1.0
SO_4^{2-}	0.5

Table 2.2 Concentration of inorganic salt species found in blood plasma[23]

A common characteristic of bioactive glasses and glass-ceramics is the formation of a biologically active apatite layer which provides the bonding with bone including the soft tissue and hard tissue[21]. Studies also showed that 12 stages of reactions occur on the material-tissue interface, as summarized in Table 2.3 and the research showed that the microstructure of the glass-ceramics had a very uniform crystal size, ranging from 8 to 20 pm [24].

Log Time (h)		Surface Reaction Stages
100	12	Proliferation of bone
	11	Crystallization of matrix
	10	Generation of matrix
	9	Differentiation of stem cells
20	8	Attachment of osteoblast stem cells
	7	Action of macrophages
10	6	Adsorption of biological moieties in HCA layer
2	5	Crystallization of hydroxyl carbonate apatite (HCA)
1	4	Adsorption of amorphous Ca + PO_4 + CO_3
	3	Polycondensation of SiOH + SiOH → Si-O-Si
	1 & 2	Formation of SiOH bonds and release of $Si(OH)_4$
		Bioactive glass

Table 2.3 Reactions Involved in Forming a bond between tissue and Bioactive Ceramics

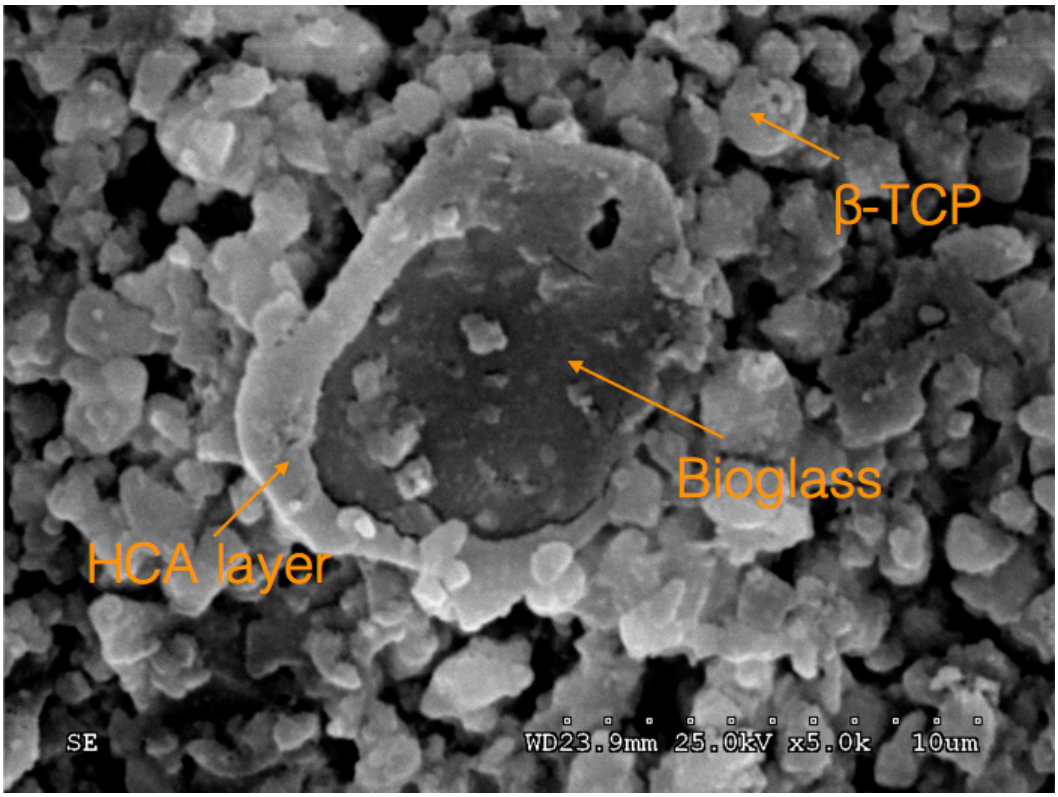

Fig 2.10 Possible the HCA layer on Bioglass 45S5 (stage5) by Hitachi S-3000N

Variable Pressure SEM

Chapter 3

Experimental Approach and Techniques

3.1 Material Characterization Introduction

In order to design a bioactive ceramic with the ability of bearing load in metabolically bone environment, it is important to understand the chemistry environments and the material characterization. The material itself need to be precisely fabricated and adapted to the needs of the local compromised bone structure but also meet the expectation of adapting the system of metabolic. In that case, a two direction of approach will be introduced in this chapter: the material properties and the in vitro study approach and techniques.

The series of experiments perform on the bioactive ceramic are design to understand the material's properties and the induced chemistry effect of the in vitro studies. First, the chemical composition of the bioceramic β-tricalcium based scaffold was characterized by X-Ray diffraction(XRD), Fourier transform infrared spectroscopy(FTIR), Raman spectroscopy and scanning electron microscopy (SEM) with energy dispersive x-ray spectroscopy (EDS) and the material's physical properties like the compression strength by material testing machine (MTS). On the other hand, the chemical response to in vitro testing by using MC3T3 cell consisting

of dissolution studies in alpha-modified Eagle's medium (αMEM), and cell culture studies with murine osteoblast precursor MC3T3-E1 cells was performed.

3.1.1 Scanning Electron Microscopy (SEM) Analysis

The Scanning electron microscopy (SEM) can create high-resolution images with a relatively large depth of focus. By combining different detection methods (secondary electrons, backscattered electrons, and x-rays), SEM can provide surface topography as well as compositional information about a sample, the atom arrangement of the bioactive β-tricalcium scaffold and showing the difference in crystal sizes of difference kind of bioactive β-tricalcium scaffold.

3.1.2 X-Ray Diffraction (XRD) Analysis

X-ray diffraction is a technique can be used to identify the crystalline materials in a system. However, the amorphous material (like 45S5 bioglass) without any crystallites can not be detected by the X-ray diffraction and will reveal a flat structure, but when the 45S5 bioglass was sintered up to 700℃, it will become crystallized[25] XRD measurements were collected in UTA's CCMB facility using the D500 Advance X-ray diffractometer with glancing angle Bragg-Brentano geometry.

3.1.3 SEM and EDS Bioactive Ceramic Composition Analysis

Scanning electron microscopy (SEM) can create high resolution of images that can see the surface topography like the grain size or the depth or focus by using all of the option of detection methods. With the EDS, the SEM machine can capture the

picture of the surface structure and with corresponding EDS spectra and maps were obtained using the Hitachi S-3000N Variable Pressure SEM with the EDAX EDS system in UTA's CCMB to determine the bioactive β-tricalcium scaffold elements composition ratios of certain mineral.

3.1.4 Fourier Transform Infrared (FTIR) Spectroscopy Analysis

At alkaline and stable pH value, TCP based scaffold progressively transforms into non- stoichiometric hydroxylated apatites. In this process the TCP base scaffold will hydrolysis to the composition $Ca_9(PO_4)_5(HPO_4)(OH)$ and apatite structure crystallization.

In order to know the formation of $Ca_9(PO_4)_5(HPO_4)(OH)$ (CDHA), the ionic groups were characterized by vibrational infrared spectroscopy, using FTIR spectrometer (Nicolet 6700, Thermo-Nicolet Corp., Madison, WI) in attenuated total reflectance (ATR) mode was used to collect FTIR spectra.

Absorption band	Wavenumber(cm^{-1})
OH^-	3500
CO_3^{2-}	1450-1640
PO_4^{3-}	1100

Table 3.1 The absorption band of detecting CDHA formation

3.1.5 Raman Spectroscopy Analysis

Raman spectroscopy provides information about molecular vibrations that used for sample identification and quantitation. The technique involves shining a monochromatic laser source on a sample and detecting the scattered light. The majority of the scattered light is of the same frequency as the excitation source. A very small amount of the scattered light (ca. 10^{-5}% of the incident light intensity) is shifted in energy from the laser frequency due to interactions between the incident electromagnetic waves and the vibrational energy levels of the molecules in the sample. With Raman spectra, it also provides the bonding information. For example, mineral phase carbonate and phosphate or matrix collagen. We can detect these bands and knowing the relative measures of bone mineral quality.

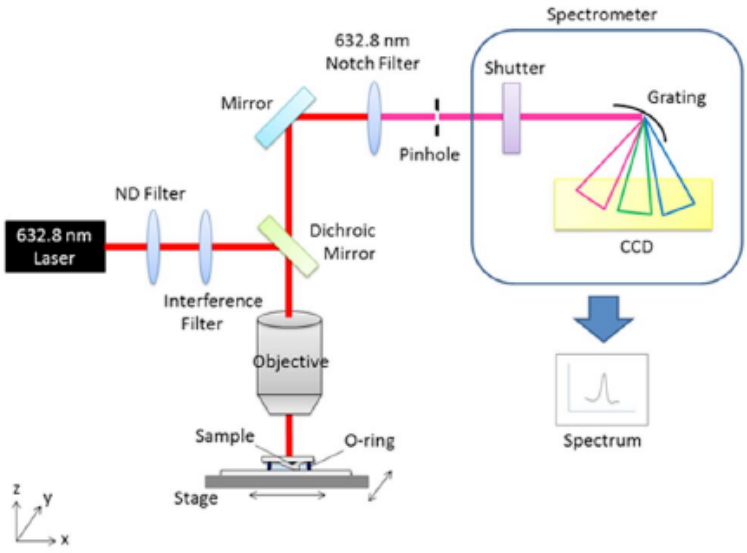

Fig3.1 Schematic diagram of the Raman platform set-up.[26]

3.1.6 Material Surface Wettability

In order to determine the hydrophilic/ hydrophobic ability of bioactive β-tricalcium scaffold sample we use goniometric machine to measure the contact angle. It quantifies the wettability of a solid surface by a liquid via the Young equation. A given system of solid, liquid, and vapor at a given temperature and pressure has a unique equilibrium contact angle. Water was used as the liquid phase. biomaterial surface is known to have a strong effect on cell response and biocompatibility[27]. Hydrophilic of the Bioceramic sample has more ability in cell adhesion. The bioactive β-tricalcium scaffold with different mixed solution of the

surface energy was linked to the interaction energy of the solid substrate with double-distilled water. Contact angles were determined at 25°C.

To analyze three-phase equilibrium and surface energy, the interfacial tensions of the solid– vapor, liquid– vapor and solid– liquid interface, and the contact angle can be related through Young's Equation. (Equation 3.1) Measurement of the two solid interfacial terms is difficult in practice and further treatment of the surface tension is considered in Good's Equation which breaks the surface energy down into a dispersive and a polar component. (Equation 3.2)

$$\gamma_{LV} \cos\theta = \gamma_{SV} - \gamma_{SL} \quad \text{Eq 3.1}$$

$$\gamma = \gamma^d + \gamma^\rho \quad \text{Eq 3.2}$$

For relatively low energy surfaces, the Owens-Wendt-Kaeble equation, which treats the total surface energy as the geometric mean of the dispersive and polar terms (Equation 3.3), is considered to be a relevant treatment of the system, and can be combined with Young's Equation to determine the polar and dispersive components of a solid's surface energy, as long as the dispersive and polar components of the surface tension of at least two probing liquids are known.[28] (Equation3.4)

$$\gamma_{SL} = \gamma_s - \gamma_L - 2(\gamma_L^d \gamma_S^d)^{\frac{1}{2}} - 2(\gamma_L^\rho \gamma_S^\rho)^{1/2} \quad \text{Eq3.3}$$

$$\gamma_{LV}(1+\cos\theta) = 2(\gamma_L^d \gamma_S^d)^{1/2} + 2(\gamma_L^\rho \gamma_S^\rho)^{1/2} \quad \text{Eq3.4}$$

3.1.7 Injectability evaluation

Injectability has been related to the viscosity of the cement, or in other words, the injection force required to deliver the cement paste. Injectability is revealed as the percentage of paste that can be extruded from a syringe, ideally in a homogeneous way under an applied force[29].Some variety of factors will lead to different consequence that different forces applied to different kind of mixture. This is a quality assessment rather a qualify results. The commercial CPC formula has the main shortcomings include the insufficient mechanical strength and poor injectability[30]. When solid/liquid segregation happened during injection worsens or even hinders the injectability[29][31]. The homogenous paste(ball mill process and binder solution included) will benefit for decreasing the extrusion force. If paste heterogeneity will increase extrusion load and might clog on the top of syringe and block the process, leaving retained paste in the syringe that contains less amount of liquid than the initial mixture.

3.2 In Vitro Testing Of Calcium Phosphate Bioactive Ceramic

3.2.1 Cell Viability Analysis

Cell viability assay is an assay to determine the ability of cells, tissue or some organ that maintain or recover viability. Cell viability is a determination of living or dead cells, based on the total cell number. Viability measurements may be used to evaluate the death or alive cells. Viability still can prove treatments benefit for cells or not in a lack of serum environment. Example of viability testing in medicine is the analysis of cells in populations where cells are routinely destroyed and this can be shown that whether the cell living environment (treated with medicine or some biomaterial) is suitable for cell to grow.

3.2.2 Cell Proliferation Analysis

Cell proliferation assay is pretty similar to cell viability assay on the concept of cell study. The only difference is the serum was treated in the medium. The serum can help cell to grow more and differentiated. The term cell growth is used in the contexts of biological cell development and cell division. Outside of a substrate's or scaffold's ability to form a carbonated apatite layer, the cellular response to the surface must

also be considered. Culture of the MC3T3-E1 subclone 4 osteoblast precursor cell line offers the ability to study cellular response to the surface. While the use of the MC3T3-E1 line has been well-established, primary cells from a human source such as human periosteum cells offer the chance to better establish a path to clinical relevance.

3.2.3 Cell Adhesion and Morphology Analysis

Cell adhesion is the process cells interact and attach to a surface, biomaterial or another cell, mediated by interactions between molecules of the cell surface. Cell adhesion occurs from the action of transmembrane glycoproteins, which is a kind of cell adhesion molecules (example like these proteins include selectins, integrins, syndecans, and cadherins.)[32]. Osteoclast cell adhesion depends on the presence of specific extracellular adhesive proteins and on the surface properties of a biomaterial[27]. Cellular adhesion plays an important role in biological process such as cell morphogenesis, cell differentiation and migration. Cellular adhesion is a link to cellular signaling[33]. Integrin receptors interact with the extracellular environment and direct signaling molecules to the cell's cytoskeleton at adhesion sites. The cytoskeleton is comprised primarily of actin fibers, tubulin microtubules, and

vimentin, desmin or keratin microfilaments, then interact with the surface via the focal adhesion[34].

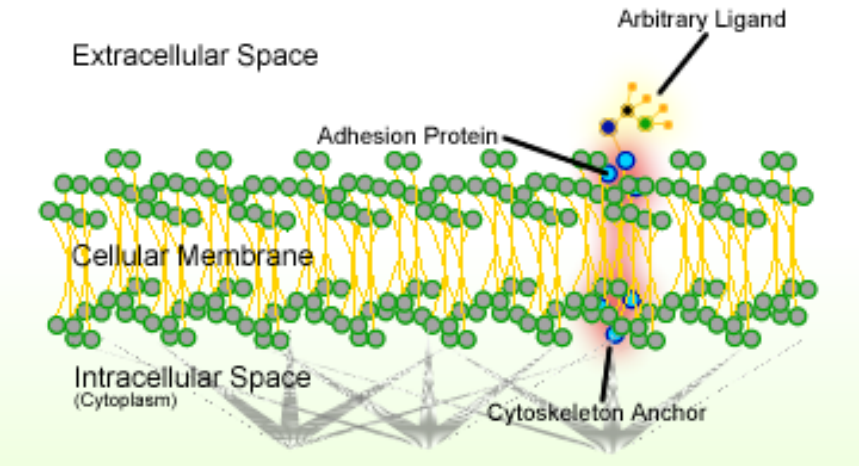

fig.3.2 Schematic of cell adhesion(https://en.wikipedia.org/wiki/Cell_adhesion)

3.2.4 Type 1 Collagen Analysis

During wound healing after bone fracture, the biosynthesis of extracellular components has been studied extensively. Microscopically, the initial response to wounding appears to be the deposition of unorganized collagen fibers (Williams, 1970; Ross and Benditt, 1961). During the Osteoblasts differentiation, the osteoblasts synthesize very dense, cross-linked collagen (Almost all of the organic component of bone is very dense collagen type I which forms dense cross-linked connection that provide better tensile strength[35]), and several additional specialized proteins which will form the organic matrix of bone. The majority part of the organic matrix is made

of collagen[36]. Well formatted cross linked collagen can differentiate to a matrix and provide well tensile strength. Then the matrix is mineralized by deposition of hydroxyapatite. Hydroxyapatite is very hard, and provides compressive strength. Thus, the collagen and mineral together are a composite material with excellent tensile and compressive strength, which can bend under a strain and recover its shape without damage. In this research, Raman spectra will use to detect the content of type I collagen. With the benefit of no cell lysis and cell fixation required. Therefore, Raman spectra can provide high sensitivity and selectivity to detect the osteogenic differentiation of MC3T3-E1 cell and we use Raman spectroscopy to detect the type I collagen.

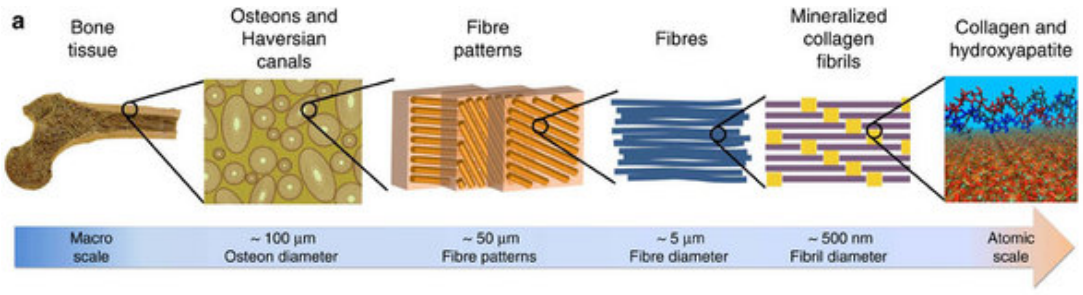

Fig 3.3 Molecular mechanics of mineralized collagen fibrils in bone[35]

Chapter 4

Design of Tri-calcium Phosphate Based Scaffolds for Biological Application

4.1 Introduction

Calcium phosphate bone cements (CPC) have attracted much attention in recent years in the medical applications area [37]. CPC offer numerous attractive advantages including osteoconductivity, biodegradability with chemical bone composition, capability to establish chemical bonds with the hard tissues, fast setting time, outstanding biocompatibility and so on[38]. Injectability and the practically isothermal in situ setting offer great opportunities to decrease the invasiveness and painfulness of surgeries, reduced recovery time and increase the overall benefits for the patient and the medical system[39]. However, the commercially available CPC formulations are not completely satisfactory[37]. The main shortcomings include insufficient mechanical strength and poor injectability. In this chapter, all the detail preparation of material, reaction of the powder synthesis, the in vitro study design will be introduced in detail in three line of experiment. Fig4.1/4.2

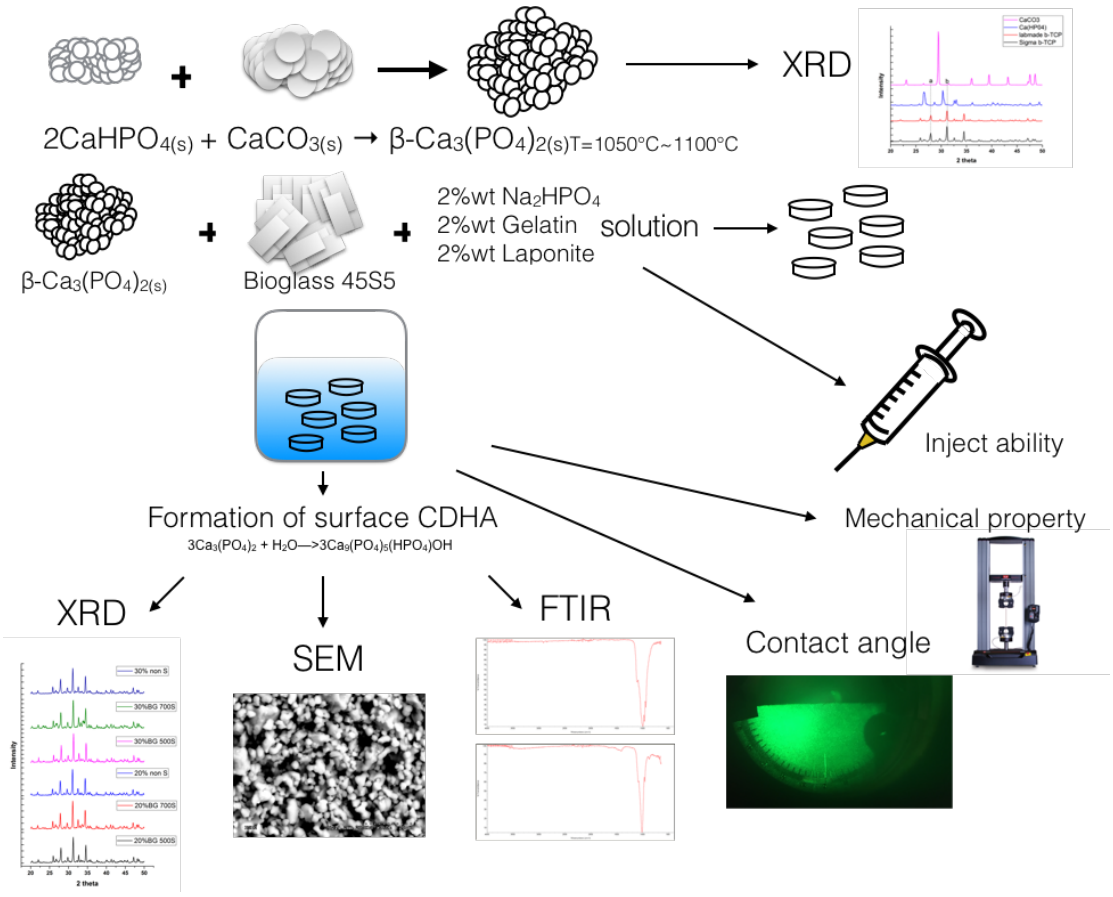

Fig4.1 The material characterization part and techniques

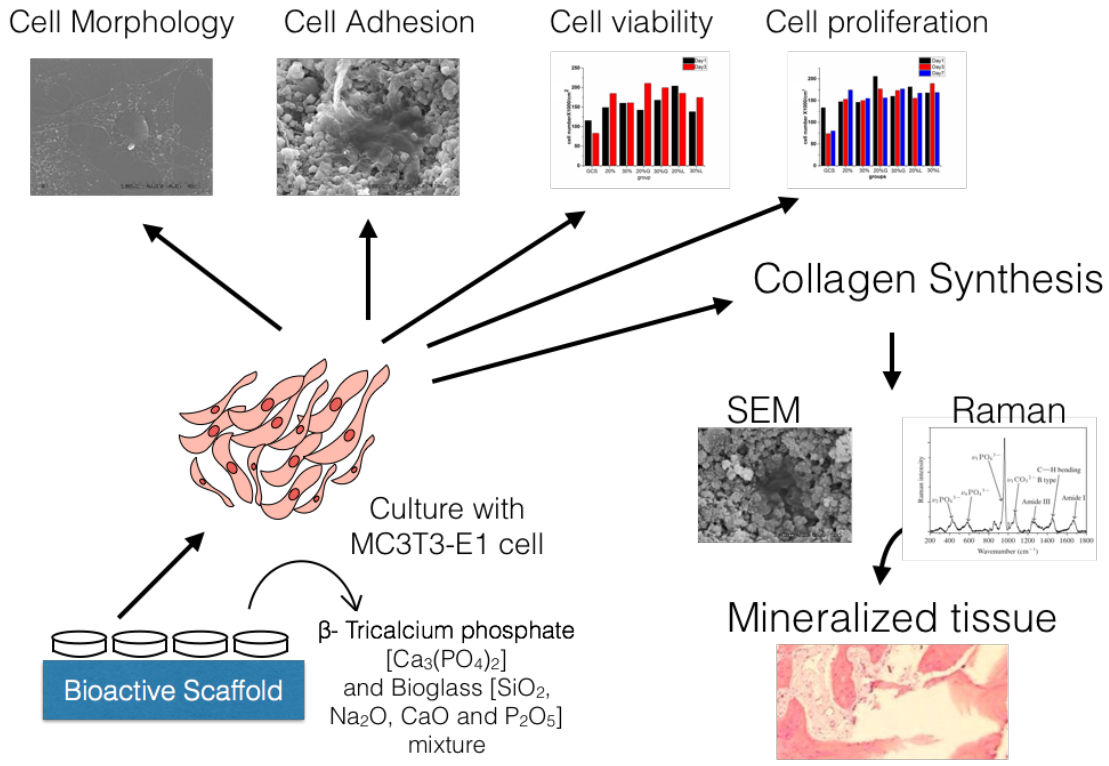

Fig 4.2 The biological part of experiment and methods

4.2 Materials and Methods

4.2.1 Synthesis of β- tricalcium Phosphate

There are three polymorphs of TCP: the low-temperature β-TCP, and the high-temperature forms, α- and α'-TCP in fig4.3. The last one lacks practical interest because it only exists at temperatures >1430°C and reverts almost instantaneously to α -TCP on cooling below the transition temperature. In contrast, β -TCP is stable at room temperature and transforms reconstructively [8][40]. Several phase equilibrium diagrams have been proposed to describe the phase relationships in the $CaO–P_2O_5$ system in fig4.3.

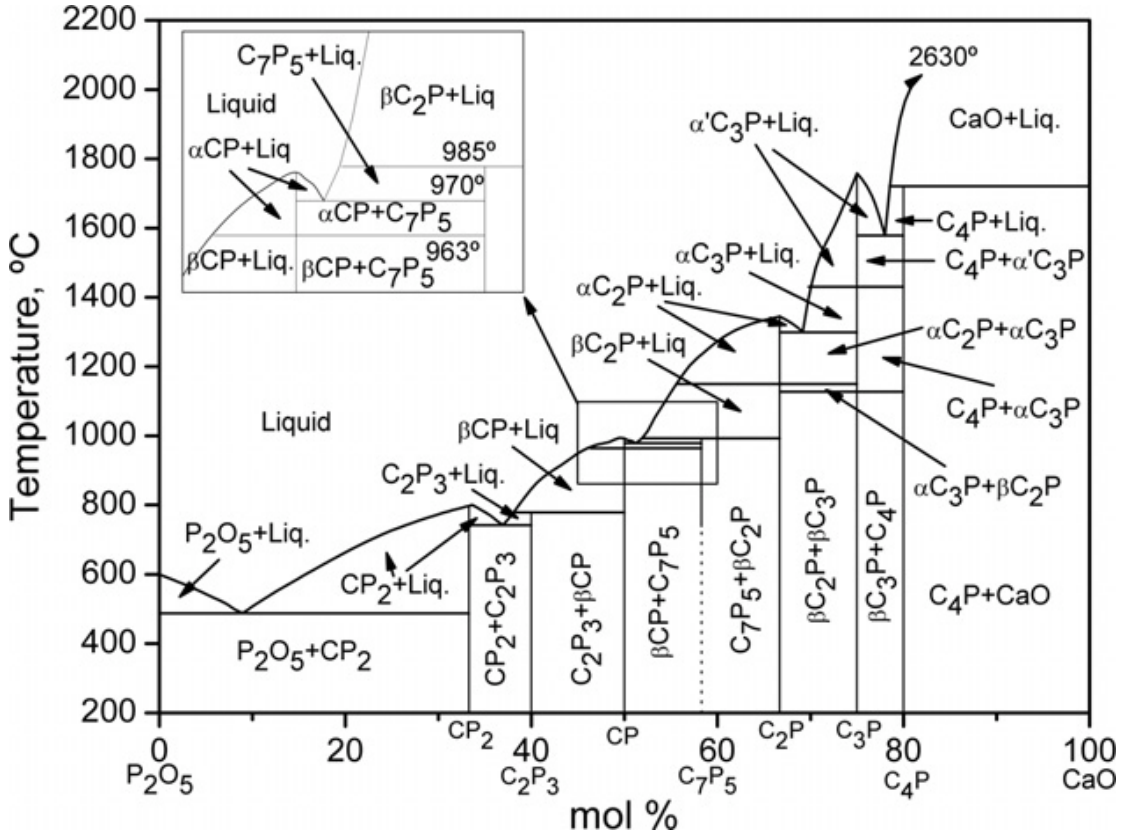

Fig. 4.3 Phase relationships in the CaO–P2O5 system according to Kreidler and Hummel[41]

β -TCP is used mainly for preparing biodegradable bioceramic shaped as dense and macro-porous granules. The beta tri-phosphate was prepared in a solid-state by the ceramic method. β -TCP was synthesized by heating a mixture of monetite (DCPA; Sigma Aldrich, United State) and calcium carbonate (CC; Sigma Aldrich, United State) in a Al_2O_3 Alumina Ceramic container with 2:1 ratio to 1050°C for 24 h with Thermolyne 6000 Muffle Furnace. The mixture was ball milled with ethanol and zirconium ball for 24h for mixing well by following the P/L ration 1:1 and P/Ball

ration 1:6. The reactant(2DCPA+CC) was dried at 60°C and heated up to 1050°C for 24h and The product (β -TCP) was ball milled for 12h to have fine powder.

$$2CaHPO_{4(s)} + CaCO_{3(s)} \rightarrow \beta\text{-}Ca_3(PO_4)_{2(s)} + CO_{2(g)} + H_2O_{(g)}$$

$$T=1050℃\sim1100℃$$

4.2.2 Scaffold preparation

The cement was produced by the mixture ball milled β –TCP and bioglass 4S5S (BG) by the proportion of 8:2(20%BG) and 7:3(30%BG) and mixing with 2wt% Na_2HPO_4(Alpha Aesar, USA), 2wt% gelatin(Sigma Aldrich, USA) and 2wt% laponite(BYK Additives LTD) solution (2%; 2%G; 2%L). Setting experiments of the liquid phase were also prepared by using deionized water. Samples were prepared by mixing the powder with the required liquid volume with P/L=1/0.35 with a mortar and pestle for 2-3 minutes and shape and quench with Teflon molds for 6mm diameter x 10mm height and 10mm diameter x 3 mm height. After setting for 30 minutes the cylinder sample will be removed from the molds and being used for the follow experiments.

4.2.3 HA formation analysis

Hydration of β –TCP powders with water or soluble phosphates in solution leads to the dissolution of calcium phosphate and deposition of a more stable, lower energy form of calcium phosphate, calcium deficient hydroxyapatite (CDHA).

$$3Ca_3(PO_4)_2 + H_2O \rightarrow 3Ca_9(PO_4)_5(HPO_4)OH$$

The 6mm diameter x 10mm height samples were soaked with Phosphate-buffered saline (abbreviated PBS) for 1,7,14 and 28 days. After soaking the certain time period. the samples were dry out and crushed for X-Ray diffraction machine (Bruker D500 X-ray diffractometer) theta - 2theta powder diffraction and FTIR machine (Thermo Nicolet 6700 FTIR Spectrometer) analysis.

4.2.4 Compression Strength Measurement

Compressive strength is the capacity of a material or structure to bear loads tending to reduce size. The testing model is ElectroForce 3300-HTAT Test Instrument the ElectroFroce systems group of Bose corpopration and the analyzing software was winTest7. Sample were prepared as a 6mm by 10 mm scaffold and all

regulation followed by ASME standard. The testing was displacement measurement. Sample will endure force until its fracture and the maximum force will be measured as the compressive strength. Compared bone will be collect from pig trabecular bone to mimic the real human bone. Al samples were sextuplicate.

4.2.5 Contact Angle Measurement

The surface energies of 20% Na_2HPO_4; 30% Na_2HPO_4; and 20% Gelatin; 30% Gelatin; 20% laponite and 30% laponite sample were determined before cell culture by the sessile drop method using one liquid phase. 10mm diameter x 3 mm height β-tricalcium scaffold were used for the contact angle by goniometric machine. The polar component of the surface energy was linked to the interaction energy of the solid substrate with double-distilled water. Contact angles were determined at 25°C with six drops placed on each sample.

4.2.6 Injectability evaluation

Injectability tests were performed as described in studies[11]. Pastes were prepared by mixing 6 g of each β –TCP and bioglass in ratio of 8:2 and 7:3 of powder

sample with an aqueous solution 2wt% Na2HPO4, 2wt% gelatin and 2wt% laponite solution using powder to liquid ratio of 0.35. The paste (6 g powder + required amount of liquid) was hand-mixed for 2 minutes and then placed into the 10ml syringe (BD, Franklin Lakes, USA, DG515805). The extrusion set was demonstrated by hands since the human force can cover the entire range of applied forces just like in a surgery and this maximum load range was selected to cover the entire range of applied forces and include all types of injection devices[42]. The extrusion was performed at room temperature (RT = 25°C) being always initiated 3 min after starting mixing the paste. The percentage of injectability was determined as the mass of the paste that explained from the syringe divided by the initial mass of the paste inside the syringe. Each injectability experiment was repeated three times and the average values were calculated.

4.2.7 Scaffold surface analysis

Desired sample were prepared with the two sputtering systems: (1) CrC-100 and (2) Hummer VI are available for coating conductive silver layers on non-conductive

samples for SEM observation, and analysis by Hitachi S-3000N Variable Pressure SEM in 25kv or 30kv voltage environment.

4.2.8 Control media preparation and cell culture

Control media (α-minimum essential medium, α - MEM; 10% fetal bovine serum, FBS and 1% penicillin-streptomycin, pen-strep). Additional supplementation of ascorbic acid (50 mg/L)(Sigma Inc, St Louis, Mo) was used in treatments for differentiation studies. Osteoblasts (MC3T3-E1 subclone 4, ATCC, Manassas, VA, passages 28–30) were cultured in 150 cm2 flasks. Once confluent, the cells were enzymatically dissociated with 5 ml trypsin (0.25%)−EDTA (0.03%) solution for the experiments. Cells were pelleted and counted (using a standard hemacytometer and inverted optical light microscope). Cells were then seeded (50000cells/cm^2) into 6-well plates and cultured for 1 and 6 days during osteoblast differentiation. The passage number of cells was maintained between 1 and 4 for all experiments.

4.2.9 Cell Viability

Cell viability media (a-minimum essential medium, a- MEM; 0.1% fetal bovine serum, FBS; and 1% penicillin-streptomycin, pen-strep) was use for testing cell viability for up to 3 days. Well plates were arranged in sextuplicate and their media changed every 2 days. Measurement of cell density was performed using the MTS assay (Promega Inc, Madison, Wisconsin). This assay is colorimetricand the intensity and the color is measured using a spectrophotometer (490nm, SpectraMax Plus, Molecular Devices,San Jose, Calif). All treatments were administered in sextuplicate. The complete experiment was also repeated for statistical

4.2.10 Cell proliferation

Cells were treated for 7 days in each treatment (no AA) for proliferation studies. Well plates were arranged such that each treatment was administered in sextuplicate and their media changed every 2 days. Measurement of cell density was performed using the MTS assay (Promega Inc, Madison, Wisconsin). This assay is colorimetricand the intensity and hue of the color is measured using a spectrophotometer (490nm, SpectraMax Plus, Molecular Devices,San Jose, Calif). All

treatments were administered in six. The complete experiment was also repeated for statistical robustness.

4.2.11 Cell Adhesion

Cells were treated for 7 days in each treatment (no AA) for cell adhesion. The sample was then collected then treated with the fixation assay. After culture, samples were removed from culture, washed in PBS twice, transferred to a fresh well plate, and fixed using 2.5% formalin (60 min), and dried using sequential alcohol dehydration 25%>50%>70%>90% and 100% ethanol–water for 5 min per concentration). Samples were dry overnight then sputtering with silver and stored in fresh well plates prior to examination by Hitachi S-3000N Variable Pressure SEM.

4.2.12 Raman Spectroscopy for collagen analysis

Raman spectroscopy is a powerful technique to study biological samples like cells without involving lengthy procedures or the need for cell lysis, staining, or fixation, but it requires a relatively high-power laser beam to overcome the inherent low Raman scattering efficiency of biological molecules[26]. The DXR Raman Microscope with laser in UTA's Characterization Center for Materials and Biology

(CCMB) (DXR, Thermo Scientific) was used to map dehydrated samples after in vitro cell cultures on the sample surface for 28 days with ascorbic acid medium to induce cell differentiation to study the impact of surface chemistry on mineral deposition. with a 532nm excitation laser at 10 mW, and a 50 μm slit. The samples were photobleached for 4 minutes prior to spectra collection and a 10 s exposure time was used.

4.2.13 ECM collagen fiber

Collagens are the most abundant protein in the extracellular matrix (ECM), and is the most abundant protein in the human body and accounts for 90% of bone matrix protein content [36]. Collagens are present in the ECM as fiber-liked proteins and give structural support to bone cells[43]. Samples was seeded and treated with 21 and 28 days with ascorbic acid medium to induce cell differentiation. Samples were fixed and dry overnight then sputtering for analyzing just mention above.

4.3 Results

4.3.1 Solid stare reaction of β- tricalcium Phosphate

β-tricalcium phosphate (β-TCP), have been intensively investigated as the cell scaffold for bone tissue engineering. However, very few qualified commercial products can be choosing from. The common accessible one was from Sigma Aldrich, United State. With the consideration of economy and stable resource of the β-tricalcium Phosphate. The method of solid state reaction was used for synthesis the β-tricalcium Phosphate and the consequence of synthesis was detect by XRD in fig 4.4.

$$2CaHPO_4(s) + CaCO_3(s) \rightarrow \beta\text{-}Ca_3(PO_4)_2(s) + CO_2(g) + H_2O(g)$$

$$T=1050^{\circ}C\sim1100^{\circ}C$$

What need to be mention was that the ball milling time of the reactant (2DCPA+CC) need to be mixing well to have complete reaction otherwise the purity will decrease due to the heterogeneous of powder. The Particle size of the β-tricalcium Phosphate was 2.43 μm as at a rough estimate with SEM PCI software indicated in fig4.5.

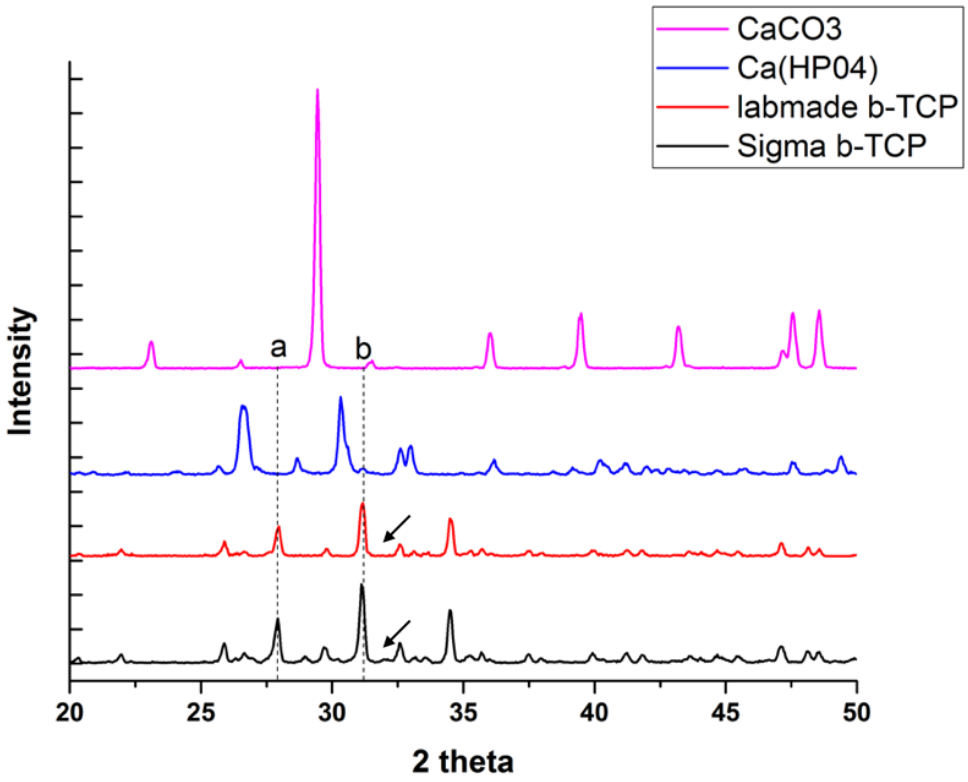

Fig 4.4 The X-ray diffraction pattern of the $CaCO_3$, $CaHPO_4$, labmade β-TCP and commercial β-TCP form Sigma Aldrich, United State.

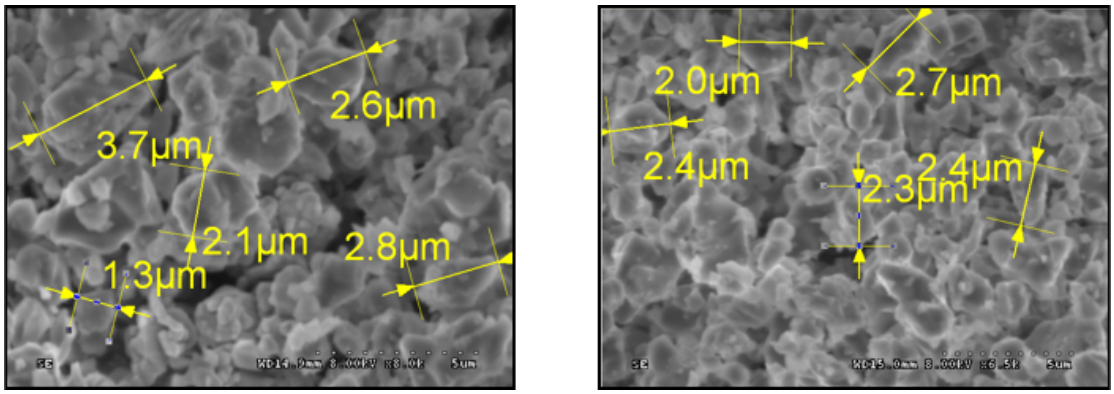

Fig 4.5 The grain structure and size of labmade β-TCP

4.3.2 Image and surface structure of bioactive scaffold

Results from quantitative imaging taken at 20kV, and 25 kV can be seen in Figure 4.6. The composite bioceramic were prepared as a disk scaffold for analyzing. β-TCP was prepared grain size around 2.43 μm by ball milling process and 30.23 μm of Bioglass 45S5 with the same method.

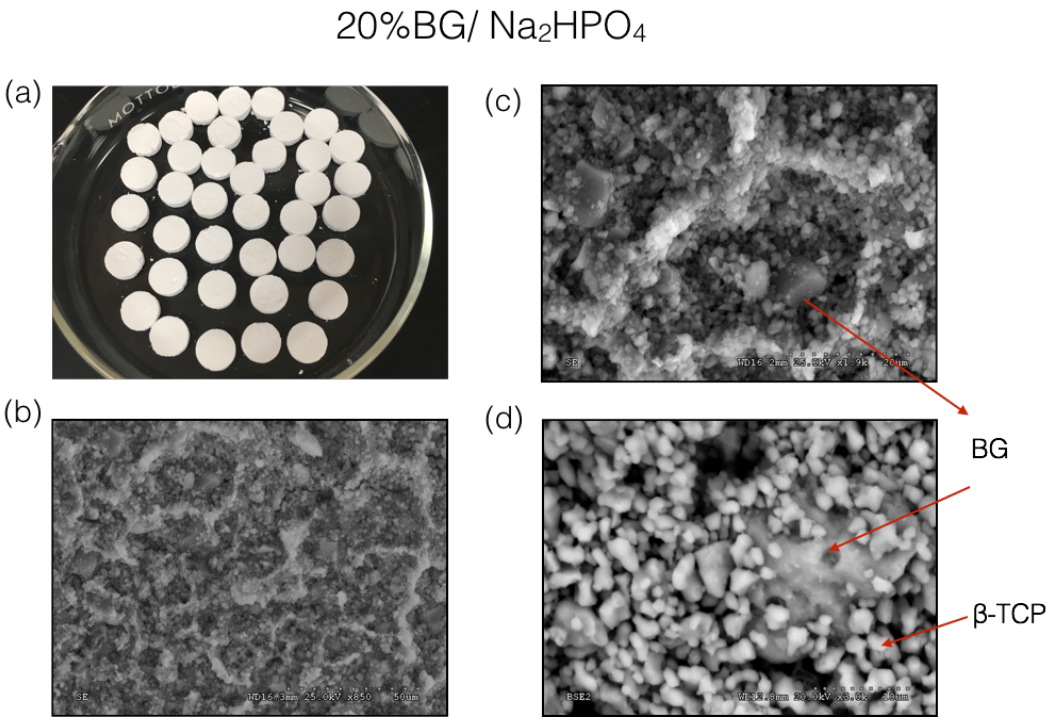

Fig 4.6 The image and surface structure of 20% Bioglass and 80% β-TCP mixture with 2wt%Na_2HPO_4 solution. (a)The scaffold image and shaped to 10mm X 3mm

bioactive scaffold. (b) The SEM image od the surface structure in magnification x850 (c) The SEM image od the surface structure in magnification x1.9k (d) The SEM image od the surface structure in magnification x3.0k. All the SEM image were taken by Hitachi S-3000N Variable SEM.

4.3.3 HA formation analysis by X-Ray Diffraction

The mineral component of human bone is mainly composed of calcium-deficient biological apatite(CDHA). they are present in bone, teeth, and tendons to provide the bone's stability, hardness, and function.[44] CDHA may be considered as HA with some ions missing. Unsubstituted CDHA (i.e. containing calcium, phosphate, hydrogen phosphate, and hydroxide ions only) does not exist in biological systems; it occurs only with ionic substitutions like Na^{+}, K^{+}, Mg^{+2}, Ca^{+2} or some carbonate, phosphate form the s biological apatite of animal and human normal and pathological calcifications. Therefore, CDHA is a very promising compound for the manufacture of artificial bone substitutes.

Hydration of β -TCP powders with water or soluble phosphates in solution leads to the dissolution of calcium phosphate and deposition of a more stable, lower energy form of calcium phosphate, calcium deficient hydroxyapatite (CDHA).[45] Equation below:

$$3Ca_3(PO_4)_2 + H_2O \rightarrow 3Ca_9(PO_4)_5(HPO_4)OH$$

All the group were soaked in PBS buffer for 1,7,14, and 28 days. After certain time period, the sample were dried out at 40 ℃ for one hour and crush to fine powder for XRD analysis. Data was recorded over the range of 20- 50˚ with a 0.04˚ step size and a dwell time of 1 second. Peak analysis was determined by the peak high and peak intensity. Higher formation of HA were shown at groups of 30% bioglass / 70% β-TCP (30%BG) with 2wt% gelatin and 2wt% laponite in fig 4.7. Quantitative peak

analysis was shown at fig 4.8.

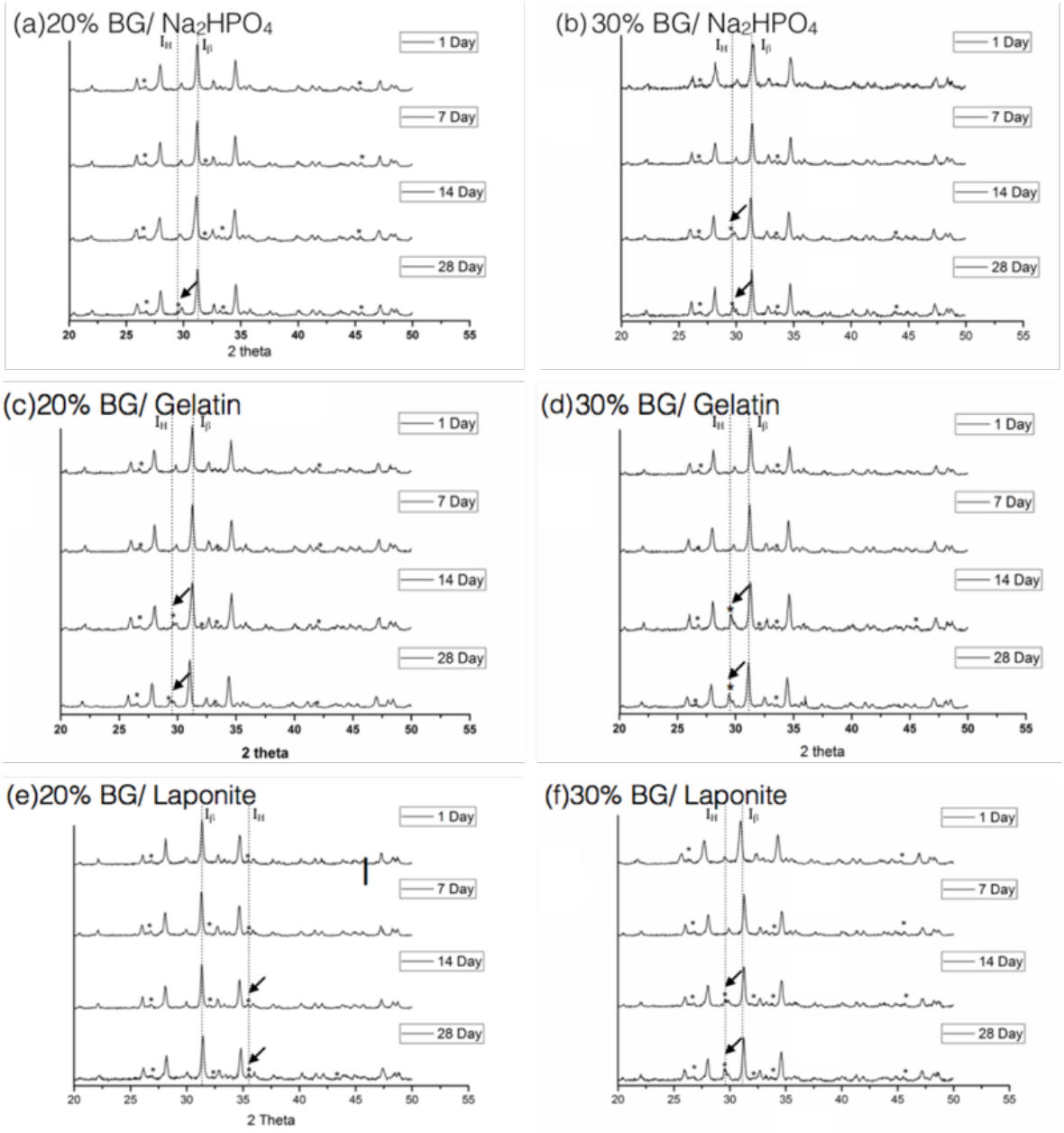

Fig 4.7 X-ray diffraction patterns of different groups and soaking days.* means the significant peak of CDHA/HA. "→"means the obvious difference between treated days. I_H: Intensity of CDHA/HA; I_β: Intensity of β-TCP. Significant formation of CDHA/HA was shown at 14-28 treated days in XRD analysis.

(a)20%bioglass and 80% β-TCP with 2wt%Na_2HPO_4 solution.(b) 30%bioglass and 70% β-TCP with 2wt%Na_2HPO_4 solution.(c) 20%bioglass and 80% β-TCP with 2wt% gelatin solution.(d) 30%bioglass and 70% β-TCP with 2wt%gelatin solution.(e) 20%bioglass and 80% β-TCP with 2wt% laponite solution. (f) 30%bioglass and 70% β-TCP with 2wt% laponite solution.

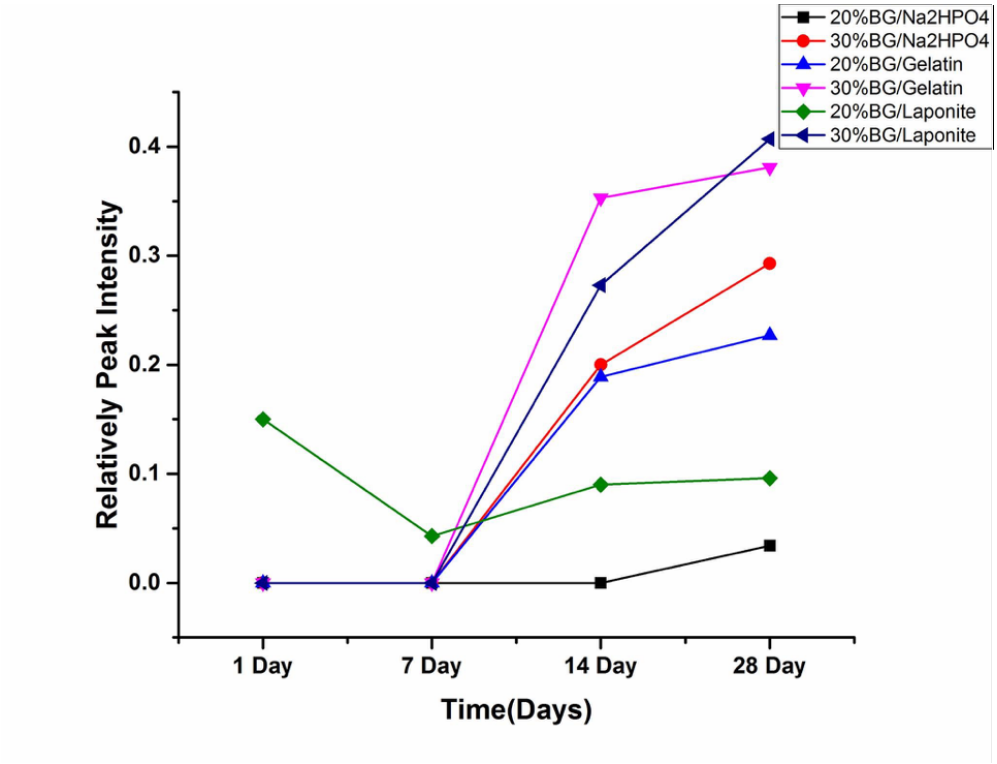

Fig 4.8 Peak Intensity of selective signature peak of β-TCP and CDHA/HA

4.3.4 HA formation analysis by Fourier Transform Infrared Spectroscopy.

The formation of HA also detected by Fourier Transform Infrared Spectroscopy. From literature[46], It is common to find substitution formula in the apatite structure and, typically, these could involve carbonate, fluoride and chloride

substitutions for either hydroxyl or phosphate groups. the characteristic IR peaks around 1450 and 1640 cm^{-1} and the peak at 873 cm^{-1} can be attributed to the vibrational frequencies of carbonate ions substituted at the phosphate site in apatite in fig 4.9. All the group were soaked in PBS buffer for 1,7,14, and 28 days. After certain time period, the sample were dried out at 40 ℃ for one hour and crush to fine powder for analyzing by Thermo Nicolet 6700 FTIR Spectrometer. Fig 4.10 shows The IR spectra of β-TCP (lab made) and HA (Sigma Aldrich, USA) and compared with The IR peaks of lab made β-TCP and commercial HA (Sigma Aldrich, USA) were also analyzed for comparison with experimental group in fig.4.11. It is obvious to found that at the first few day of soaking at the PBS, some HA/CDHA already to synthesis which is not easily to find in X-Ray diffraction.

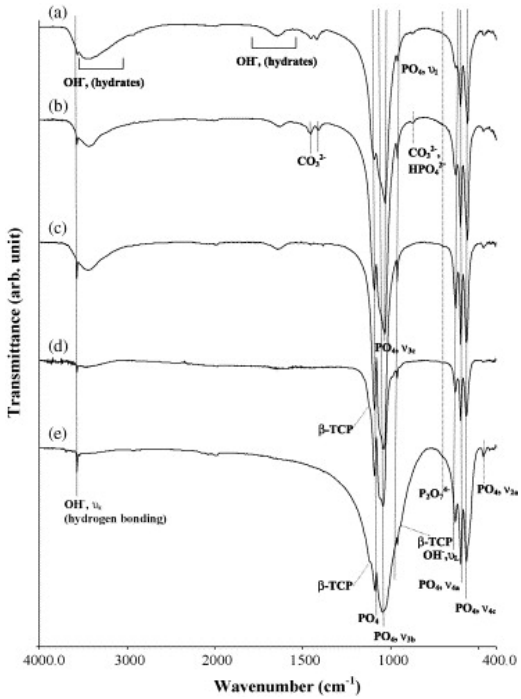

Fig 4.9 IR spectra of the HAP precipitates: (a) as-dried, (b) calcined at 700 °C, (c) calcined at 800 °C, (d) calcined at 900 °C and (e) calcined at 1200 °C.[46]

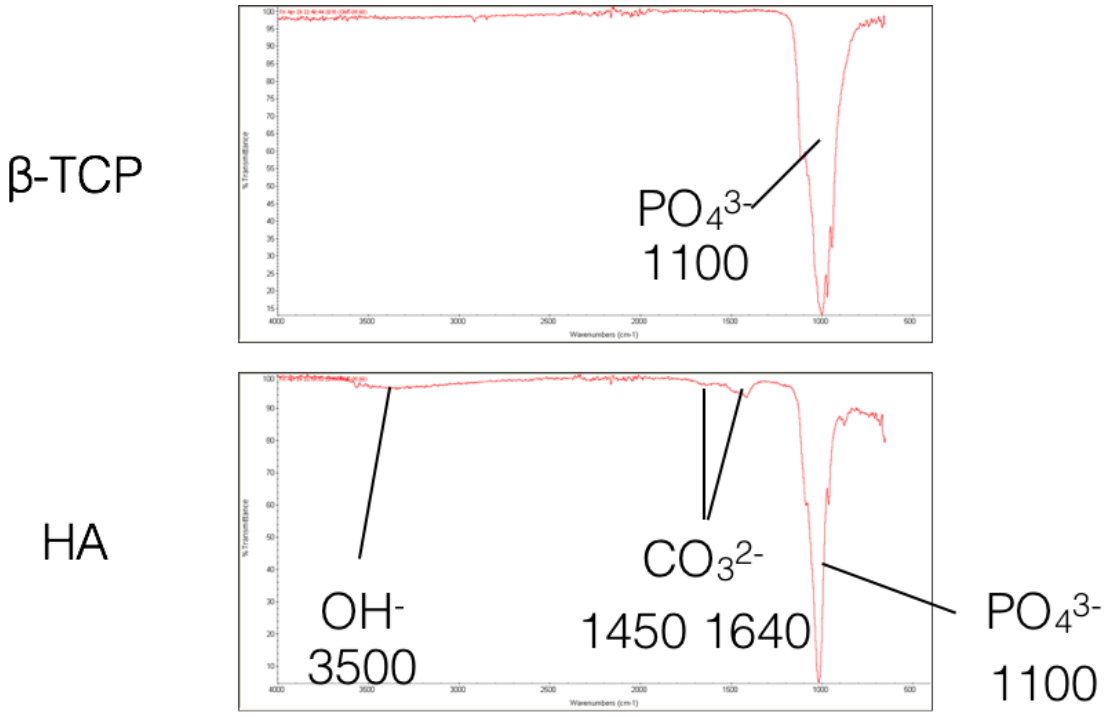

Fig 4.10 The IR spectra of β-TCP (lab made) and HA (Sigma Aldrich, USA) by Thermo Nicolet 6700 FTIR Spectrometer.

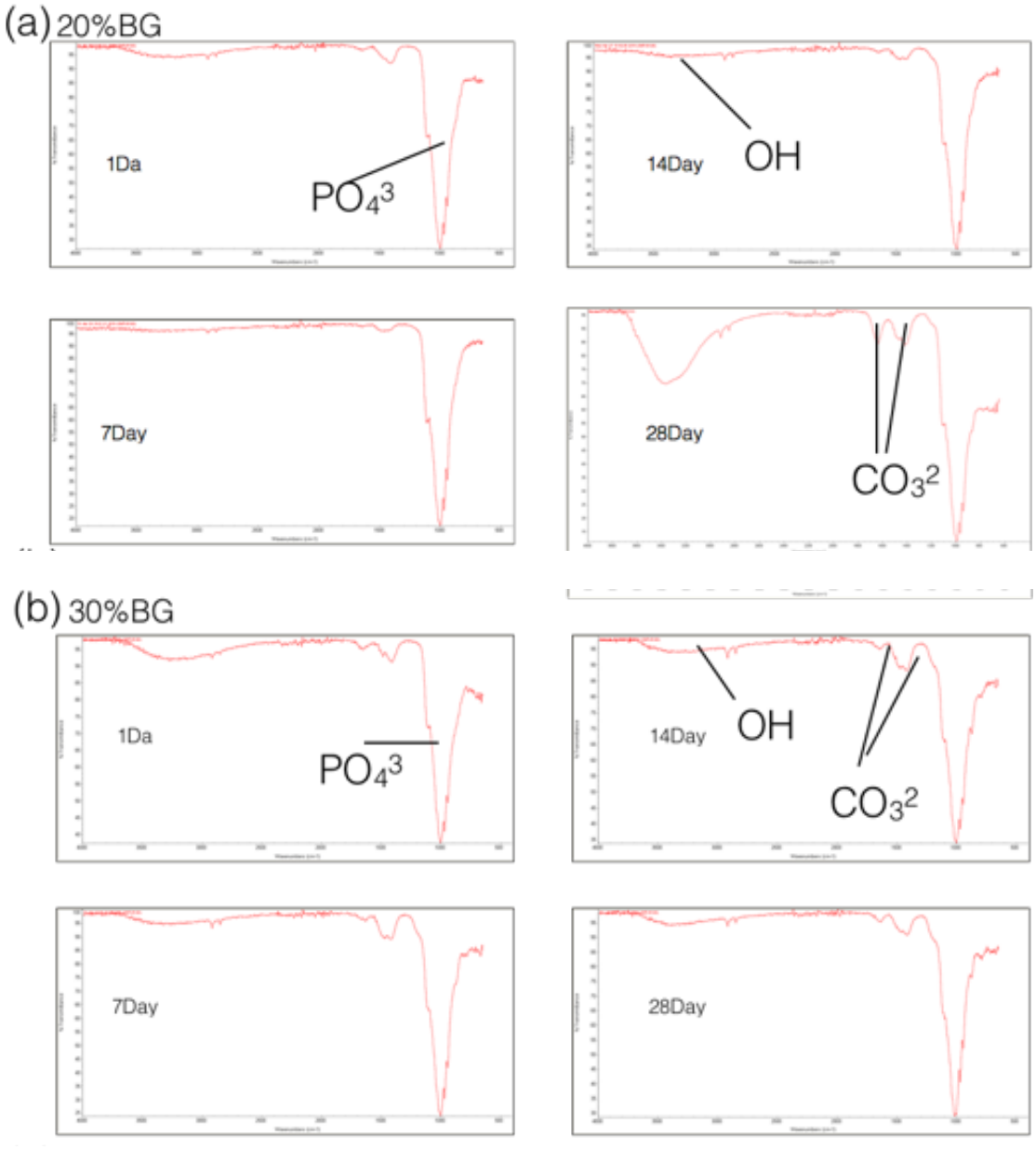

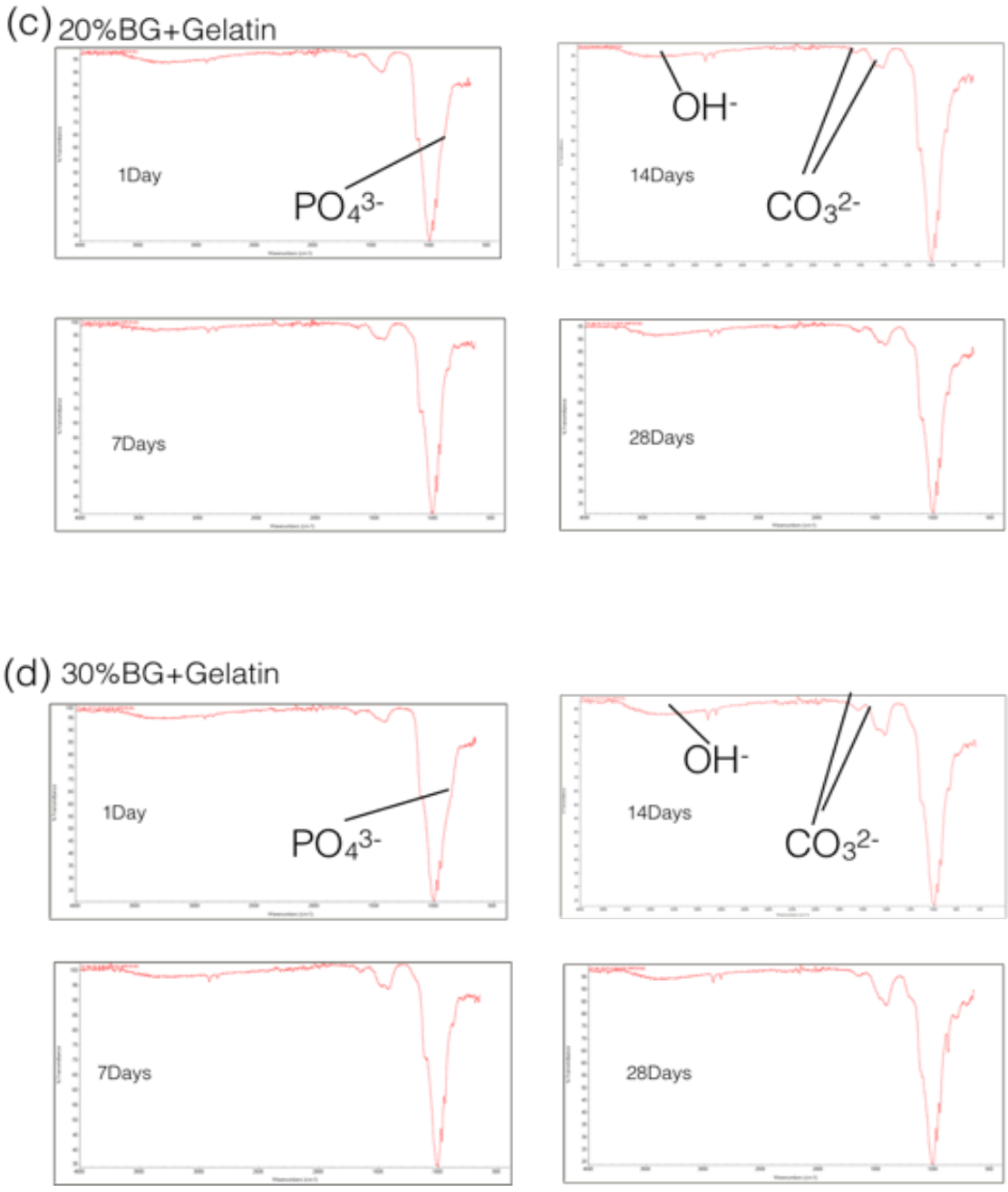

Fig 4.11 The IR spectra of different groups and setting days by Thermo Nicolet 6700 FTIR Spectrometer. The 1450 and 1640 cm⁻1(carbonate ions) and the peak at 3500 cm^{-1} can be attributed to the hydroxyl or 1100 cm^{-1} for phosphate groups. (a)20%bioglass and 80% β-TCP with 2wt%Na_2HPO_4 solution. (b) 30%bioglass and 70% β-TCP with 2wt%Na_2HPO_4 solution. (c) 20%bioglass and 80% β-

TCP with 2wt% gelatin solution.(d) 30%bioglass and 70% β-TCP with 2wt%gelatin solution.(e) 20%bioglass and 80% β-TCP with 2wt% laponite solution. (f) 30%bioglass and 70% β-TCP with 2wt% laponite solution.

4.3.5 Contact angle

The contact angles, as determined by a sessile drop technique for the probing liquids (DI water) to the top of selective scaffold. The demonstrate picture are shown at fig 4.12 The angle measurement result are shown in Table 4.1, the angle of all the groups were below 13.0 ° which means the scaffold are so hydrophilic. With the advantage, we have basic hypothesis that the β-TCP bioglass composite scaffold may benefit for cell to grow since the more affinity to water sometimes means the more biocompatible to cells. The water contact angle increases in content from the mixed solution sodium hydro phosphate around 12.5 ± (20.7~1.52). The angle of gelatin and laponite were smaller that from (5.67~5.83) ± (1.5~1.33)˚ and (7.5~8.3) ± (1.38~1.97) ˚.

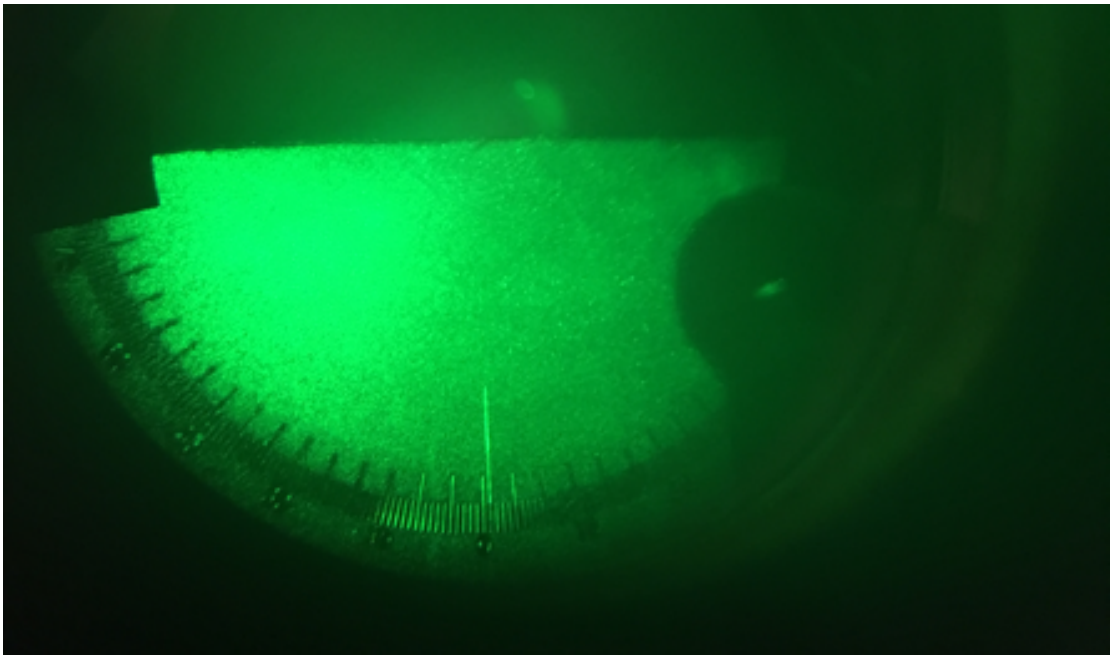

Fig 4.12 The microscope view of the measurement of contact angle. The drop(Right) will touch the scaffold surface(Top) and the angle will be measured in scale.

Materials/Solution	water	
20% Na_2HPO_4	12.5 °	(2.07)
30% Na_2HPO_4	12.5 °	(1.52)
20% Gelatin	5.67 °	(1.5)
30% Gelatin	5.83 °	(1.33)
20% Lapointe	7.5 °	(1.38)
30% Lapointe	8.3 °	(1.97)

Table 4.1 The contact angle measurement between groups (All group were determined by six sessile drops of DI water)

4.3.6 Injectability

Injectability offers great opportunities to decrease the invasiveness and painfulness of surgeries, reduced recovery time and increase the overall benefits for the patient and the medical system. The paste (6 g powder + required amount of liquid) was hand-mixed for 1 min and then placed into the syringe. The extrusion set was placed in the weighing machine before and after extrusion. The extrusion was performed at room temperature being always initiated 3 min after starting mixing the paste. The percentage of injectability was determined as the mass of the paste that explained from the syringe divided by the initial mass of the paste inside the syringe. The 30%bioglass and 70% β-TCP with 2wt%gelatin solution performed the best injectability among groups up to 95.6% of paste extruded shown in table 4.2 and fig 4.13, and the second is the 30%bioglass and 70% β-TCP with 2wt% laponite solution up to 83% paste extruded. It also indicated that the 30%bioglass' group perform a better injectability than the 20% groups. The possible reason might be the packing density of pure β-TCP will induce clogged on the syringe. Since the packing density of 20% groups was greater than 30% group (β-TCP particle size was significant

smaller then bioglass), the 30% groups' injectability was all better then the 20% group.

Groups	Paste before extruding(g)	Remaining paste after extruding(g)	Extruded paste(g)	Injectability(% extruding)
20%BG/Na_2HPO_4	6.92 6.89 6.56	4.59 4.7 4.6	2.33 2.19 1.96	31.8%
30%BG/Na_2HPO_4	6.99 6.77 6.56	3.32 3.31 3.2	3.67 3.46 3.36	51.6%
20%BG/2wt%G	6.36 6.68 6.66	2.0 2.1 2.0	4.36 4.68 4.66	69.5%
30%BG/2wt%G	6.93 6.5 6.78	0.3 0.31 0.28	6.93 6.19 6.5	95.6%
20%BG/2wt%L	6.91 6.55 6.78	3.0 3.3 3.12	3.91 3.25 3.66	53%
30%BG/2wt%L	6.79 6.78 6.55	1.1 1.1 1.2	5.69 5.68 5.35	83%

Table 4.2 The injectability among all groups. The test was operated by triplicate. And the 30%Gelatin groups has the best performance up to 95.6%

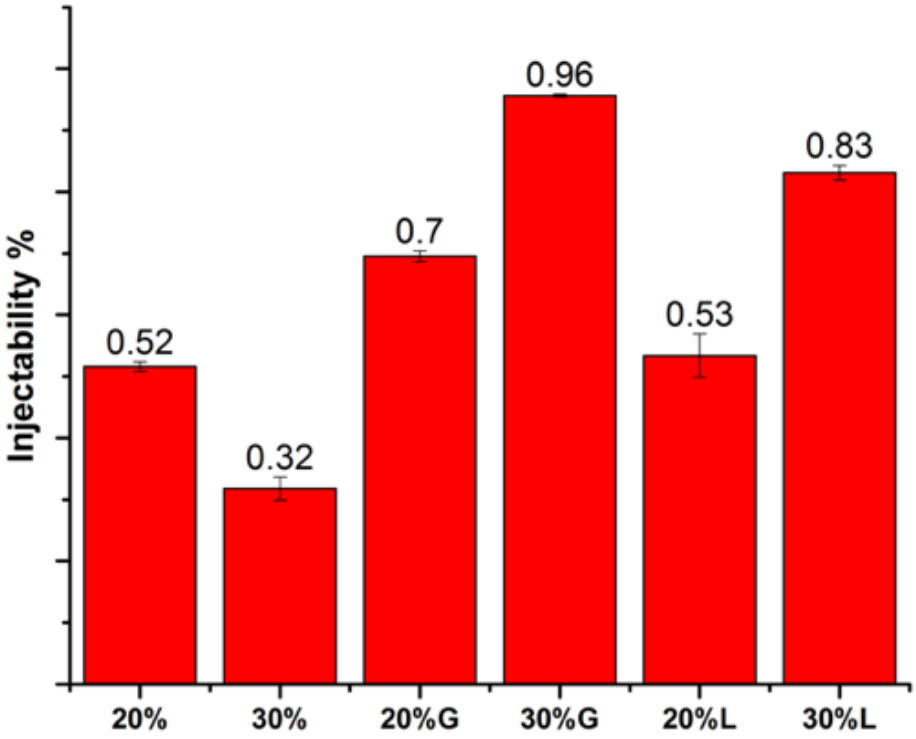

Fig 4.13 The injectability of all groups. 20%bioglass and 80% β-TCP with 2wt%Na_2HPO_4 solution; 30%bioglass and 70% β-TCP with 2wt%Na_2HPO_4 solution; 20%bioglass and 80% β-TCP with 2wt% gelatin solution; 30%bioglass and 70% β-TCP with 2wt%gelatin solution;20%bioglass and 80% β-TCP with 2wt% laponite solution and 30%bioglass and 70% β-TCP with 2wt% laponite solution.

4.3.7 Mechanical Property Testing

The compressive strength of the material would correspond to the stress at the red point shown on the curve. In a compression test, there is a linear region where the material follows Hooke's Law. $\sigma = E\varepsilon$ where this time E refers to the Young's Modulus for compression. The scaffold will endure a displacement testing(1.3mm/min) until fracture at their compressive strength limit and the maximum force will be measured as the compressive strength. To determine whether this β-TCP bioglass composite will be compatible to real bone, the pig trabecular bone will be collect by a driller to collect as the sample size of the scaffold groups. The scaffold was prepared by 6mm x 10mm followed by the ASTM standard XXX regulation. Bioglass had been proved to benefit to mechanical property and was shown at fig 4.3.7. At first day, the samples' mechanical was far from the pig trabecular bone may be the setting time of β-TCP bioglass composite still undergoing, but after 28 days among all groups can be compatible to the trabecular bone especially the 30%Gelatin has the maximum compressive strength bearing ability up to 1.36 times to pig trabecular bone in fig 4.15

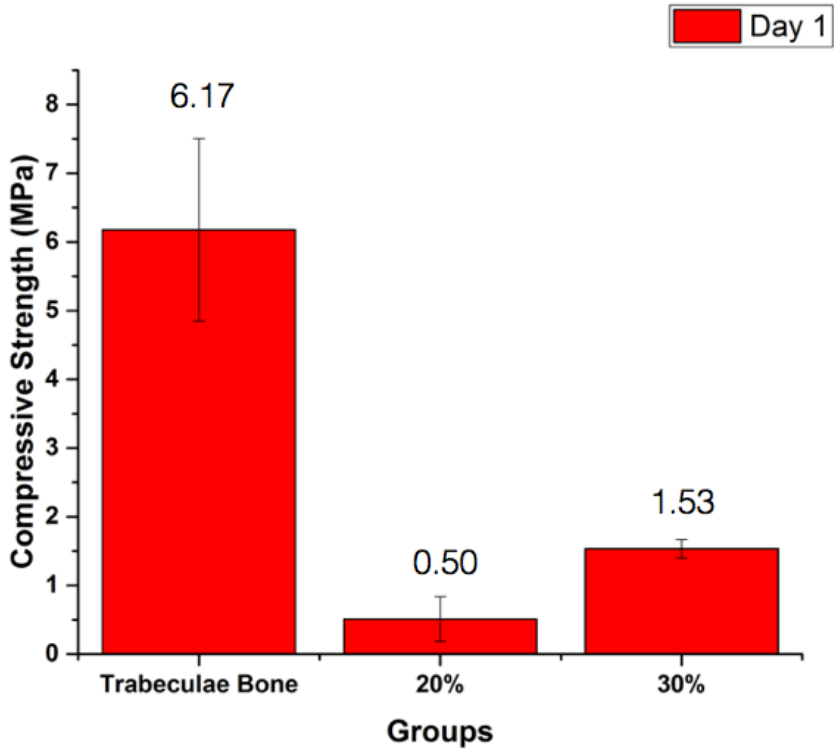

Fig 4.14 The 30% bioglass has better mechanical property around 3 times to 20% group in day 1.

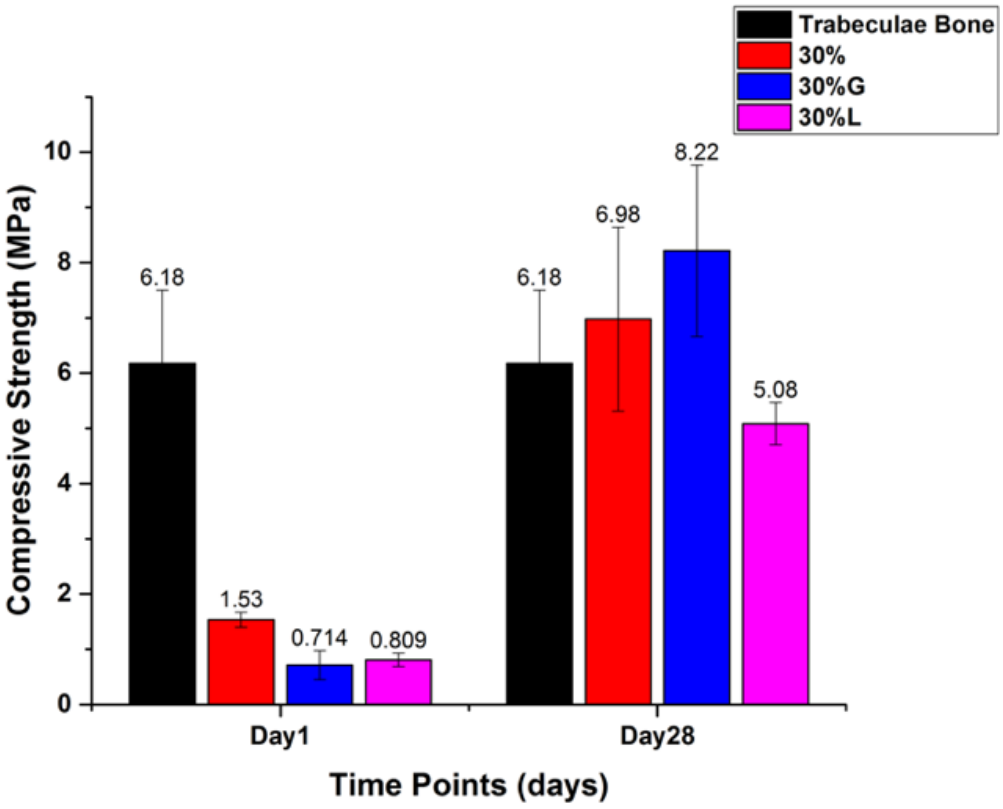

Fig. 4.15 The compressive strength of β-TCP bioglass composite at day 1 and day 28.

4.3.8 Cell Adhesion and Cell morphology

It is well known that during the contact between a cell and a biomaterial, the information will be transferred from the material surface to the cell and this contact is so called" cell adhesion". Cell adhesion is crucial for the assembly of individual cell into the three-dimensional tissues or even some system and organ. Cells do not simply "stick" together to form tissues, but rather are organized into very diverse and highly

distinctive patterns. β-TCP bioglass composite scaffold with different kinds of proportion of Bioglass and bonding solution shows great cell adhesion in figure 4.16

The picture was taken after 7 days the cell seeded by Hitachi S-3000N Variable SEM in 25kV.

(a)

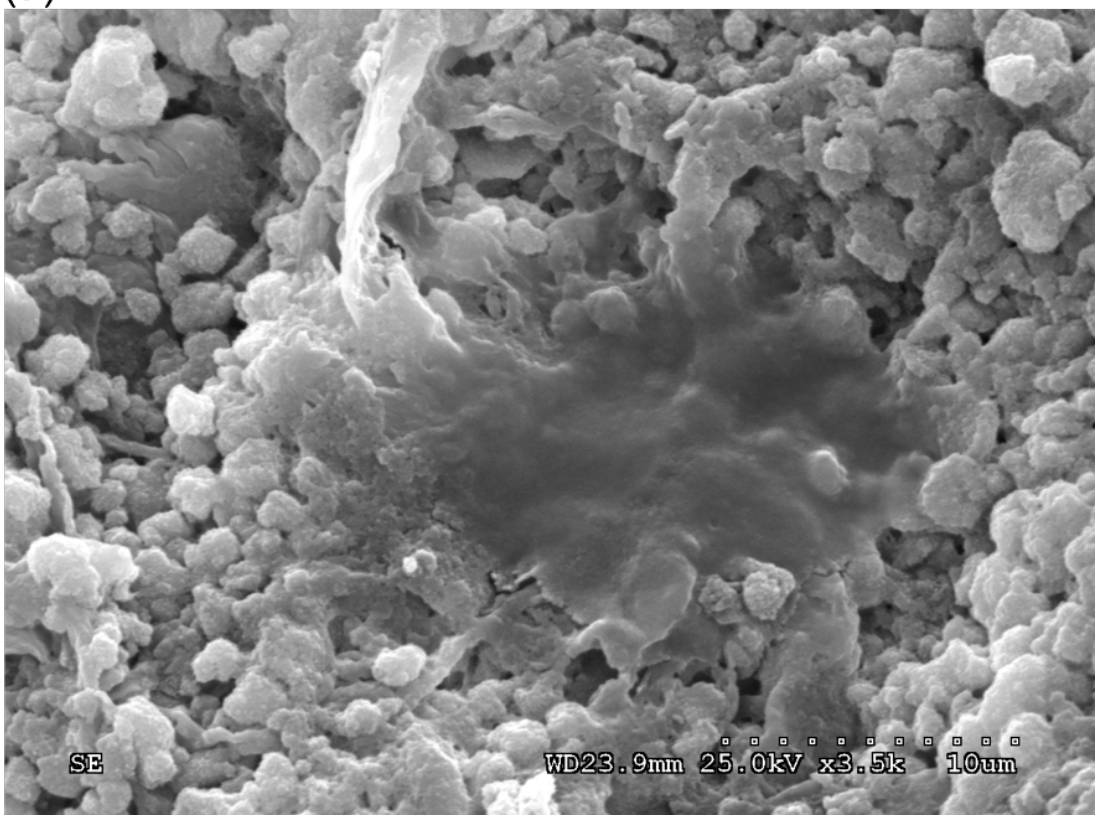

(b)

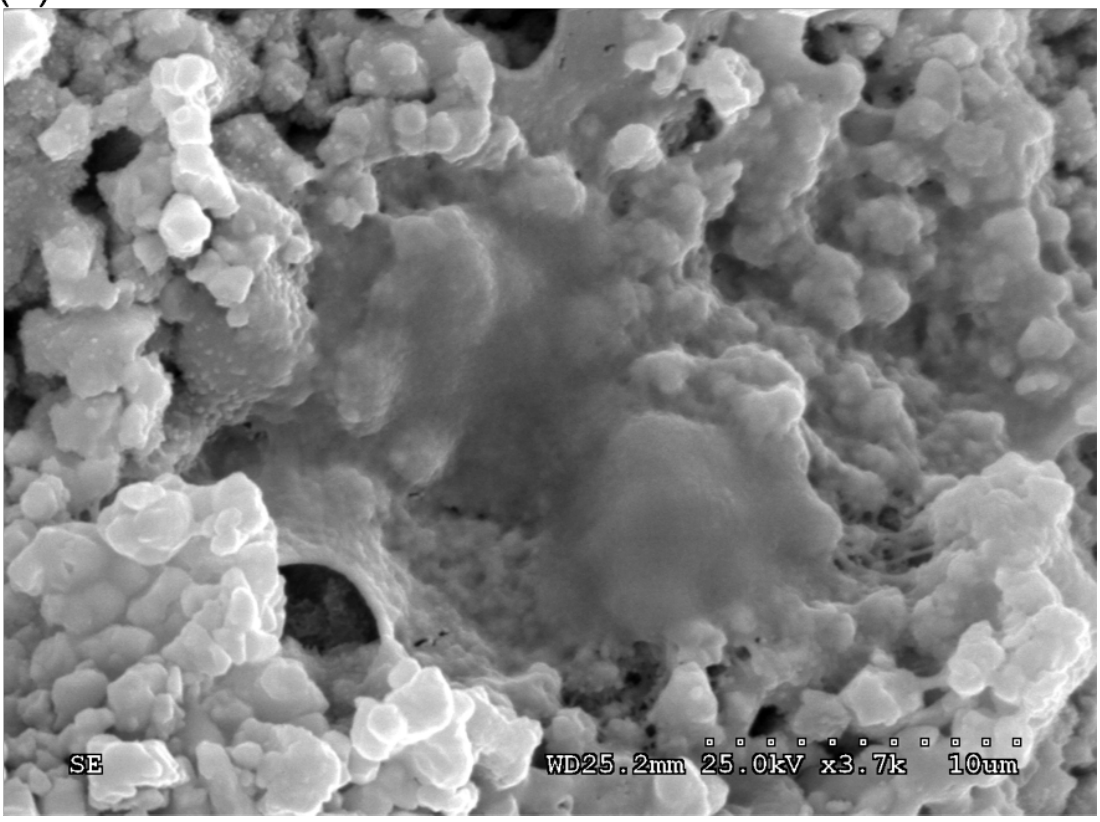

Fig 4.16 The MC3T3-El subclone4 cell attach to the β-TCP bioglass composite scaffold in (a) The sodium hydro phosphate scaffold in WD 23.9mm and (b)gelatin scaffold in WD 25.2mm under 25Kv

4.3.9 Cell Viability

Measurements for cell viability are used to evaluate the viable of cells. Cell viability assays are also often useful to determine optimal growth conditions of cell populations maintained in culture. MTS reagent was used in the cell viability measurement. The assay is based on the reduction of MTS tetrazolium compound by viable cells to generate a colored formazan product (purple) that is soluble in cell

culture media. This conversion is thought to be carried out by NAD(P)H-dependent dehydrogenase enzymes in metabolically active cells. The formazan dye produced by viable cells can be quantified by measuring the absorbance by 490nm, SpectraMax Plus, Molecular Devices (San Jose, Calif). All the group were treated with regular medium(a-minimum essential medium, a- MEM; 0.1% fetal bovine serum, FBS; and 1% penicillin-streptomycin, pen-strep). At First day measurement we can found that all the scaffold group reflect a better viability(~2X) to control glass cover slip group in fig4.17. The 20%BG/2wt% laponite decrease to 75% of the first day that might because cell reach its maximum density and the pressure from the environment cause the reduce of cell number r maybe some technical issue. This part need to be examined again. But over all, the viability shows that the β-TCP bioglass composite can prove a great substrate for cell to attach and stay alive. This experiment can be mimic when bone defect happens, the circumstance of cell reacts with the scaffold to determined whether this scaffold can show a basic biological property.

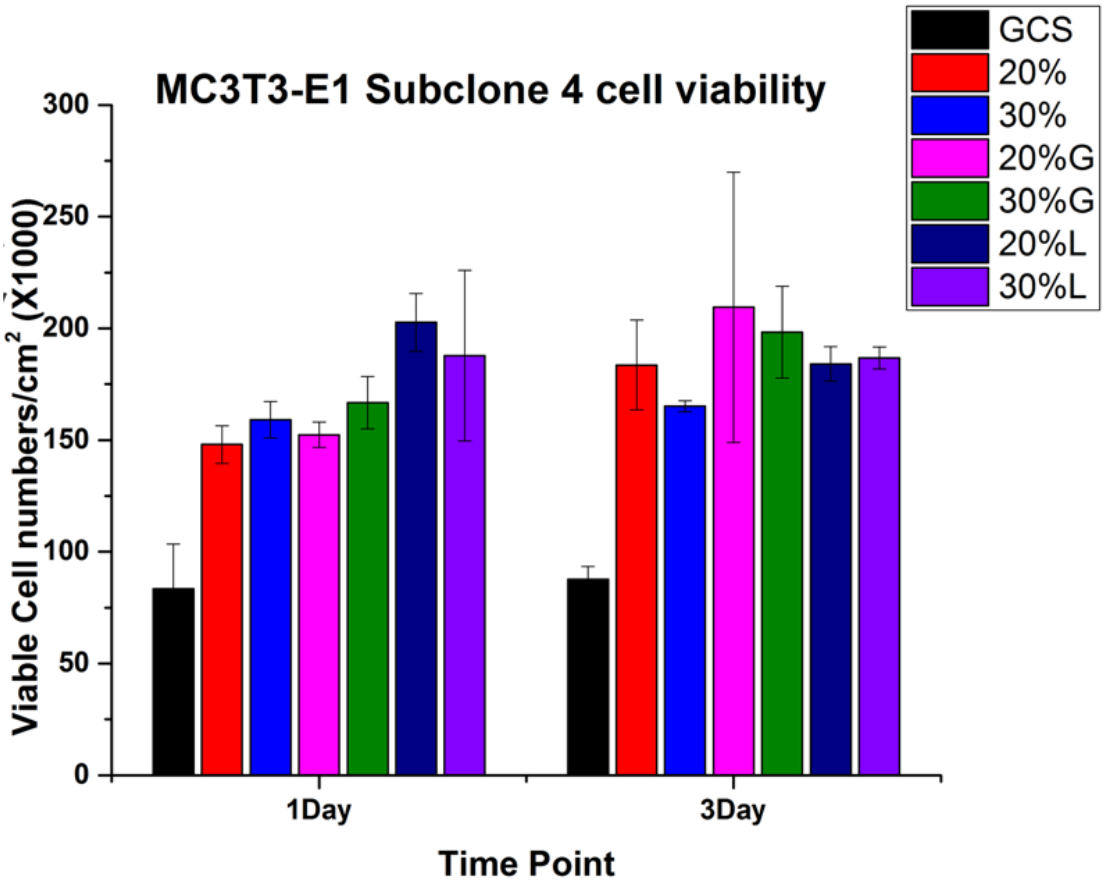

Fig 4.17 The cell viability of the MC3T3-E1 subclone 4 cell with glass cover slip and scaffold groups. (20%--20%Bioglass/80% β-TCP with 2wt% Na_2HPO_4; 30%--30%Bioglass/70% β-TCP with 2wt% Na_2HPO_4 solution; 20%G--20%-20%Bioglass/80% β-TCP with 2wt% Gelatin solution; 30%G--30%Bioglass/70% β-TCP with 2wt% Gelatin solution; 20%L-- 20%Bioglass/80% β-TCP with 2wt% laponite solution and 30%L-- 30%Bioglass/70% β-TCP with 2wt% laponite solution)

4.3.10 Cell proliferation

Cell Proliferation Assay measures the cell proliferation rate and the metabolic activity of cells and the method is similar to cell viability assay on the concept of cell study. The only difference is the serum was treated in the medium. The serum can help cell to grow more and differentiated. Medium (α-minimum essential medium, α-MEM; 10% fetal bovine serum, FBS; and 1% penicillin-streptomycin, pen-strep) was use for testing cell viability for up to 7 days. It can be found that the 30% gelatin and 30% laponite growth stably and larger cell number compare to the GSC group in 1-7 days in fig 4.18. That day one sometimes can detect large cell number means cell grow so fast during the first day. After day 1, the cell environment was reach to its limit and cell cannot grow as fast as the day 1. The real performance of the cell proliferation would be stabilized, and the β-TCP bioglass composite can let cell to grow and forming some vascular even lead to more differentiation of bone cells

Some problems were found in this MTS assay is that some precipitated of formazan on the scaffold occasionally in fig 4.19. In this case, the error will influence the absorbance and need to be eliminated from the group.

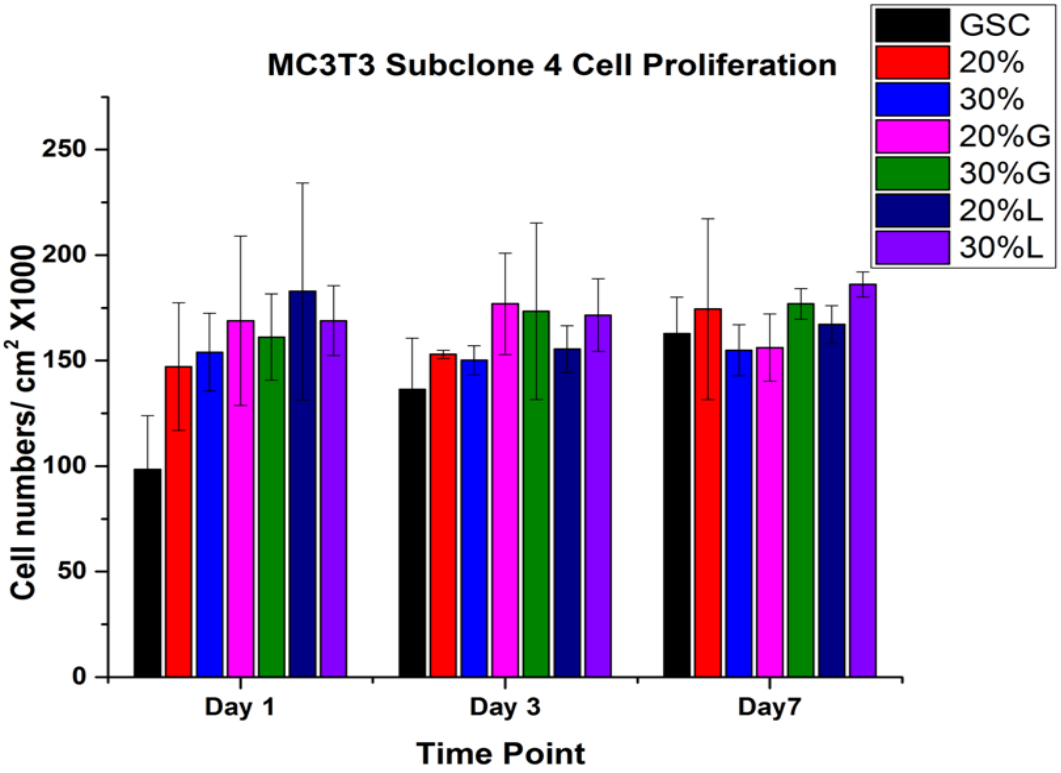

Fig 4.18 The relative cell growth of the MC3T3-E1 subclone 4 cell with glass cover slip and scaffold groups. (20%--20%Bioglass/80% β-TCP with 2wt% Na_2HPO_4; 30%--30%Bioglass/70% β-TCP with 2wt% Na_2HPO_4 solution; 20%G--20%-20%Bioglass/80% β-TCP with 2wt% Gelatin solution; 30%G--30%Bioglass/70% β-TCP with 2wt% Gelatin solution; 20%L-- 20%Bioglass/80% β-TCP with 2wt% laponite solution and 30%L-- 30%Bioglass/70% β-TCP with 2wt% laponite solution)

Fig 4.19 precipitated of formazan on the scaffold

4.3.11 Collagen Analysis by Raman Spectroscopy

Raman spectroscopy offers the ability to study bonding information, and, unlike more the common FTIR spectroscopy technique, using raman spectroscopy in biological investigations presents several advantages, especially when compared to IR technique. Raman micro spectroscopy is able to probe samples at the micrometer scale, and water causes very little interference. Several Raman measures of bone quality have been developed. Most bands observed in a Raman spectrum of bone can be assigned to mineral phase carbonate or matrix collagen, and these bands can be

used to measures of bone differentiate quality. The major collagen bands were always observed around 1200–1300 cm^{-1} and 1600–1700 cm^{-1} (amide III and I, respectively), and 1400–1500 cm^{-1} (CH groups). Additional information was obtained from the Raman signature of different amino acids observed in the spectra. The phenylalanine (Phe) band, for example, was identified in all spectra at 1010 cm^{-1}. All spectra were shown at fig4.20 and Table 4.3

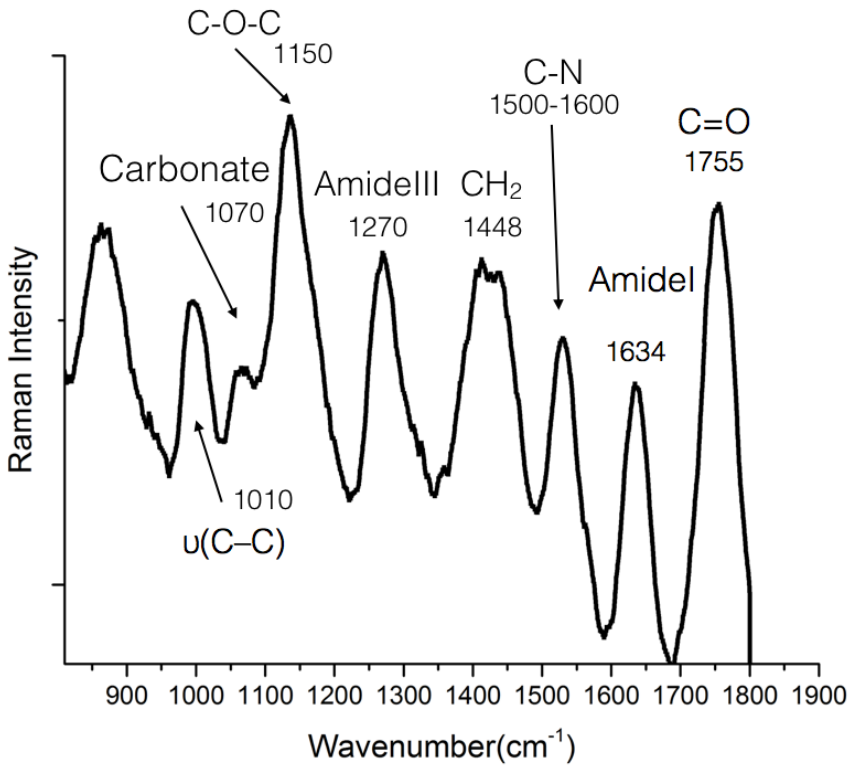

Fig 4.20 28 days after seeding MC3T3 cells sample. Raman bands in bone

spectra were consistent with those found in the carbonated apatite spectrum around

1070 cm^{-1}. The major collagen bands were always observed around 1200 ~1300 cm^{-1} (amide III) and 1600 ~1700cm^{-1}(amide I). 1448 cm^{-1} bending and stretching modes of CH groups. The phenylalanine (Phe) band was identified in all spectra at 1010 cm^{-1}. The CH bands frequently overlapped the lipid bands.

Raman shift cm^{-1}	**assignment**	**comment**	**Ref**
1010	**υ(C–C)**	**Phenylalanine**	[47]
1070	**Carbonate**	**Overlaps with component of $υ_3PO_4^{3-}$**	[48][49]
1150	**υ(C–O–C)**	**Tyrosine, phenylalanine**	[48][47]
1270	**AmideIII**	**Protein a-helix**	[26][47]
1448	**CH_2**	**Protein CH_2 deformation**	**[44][45]**
1500-1600	**C-N**	**sp^2 chain species**	[48][50]

1634	**AmideI**	**Strongest amide I component, polarization sensitive**	[47], [48]
1700-1800	**C=O**	**strong InfraRed**	[48]

Table 4.3 Raman spectroscopic band assignments for bone mineral and matrix components

4.3.12 Collagen Analysis by SEM microscope

Dermal repair tissue shows a progressive increase in collagen content which may be related to the cell differentiation and bone repair. The ECM is composed of an interlocking mesh of fibrous proteins and glycosaminoglycan. It includes Proteoglycans(like heparan sulfate, Chondroitin sulfate and keratan sulfate), Non-proteoglycan polysaccharide like the Hyaluronic acid and the most important one fibers such as collagen fiber or some elastin fiber

After the proliferative phase, the synchronization medium (α-minimum essential medium, α- MEM; 50mg/L ascorbic acid; 10% fetal bovine serum, FBS; and 1% penicillin-streptomycin, pen-strep) was treated to induce the collagen synthesis. The

formation of collagen fibers was observed by scanning electron microscopic after 21 and 28 days in fig 4.21 of cell culture and this process appears corresponding to bone remodeling. The observation of collagen fibril-bundles was shown in fig 4.22. Compare to some researches[43][51] can obtain very similar result for different stage of collagen development, the single fiber, cross-linked collagen and a matrix one.

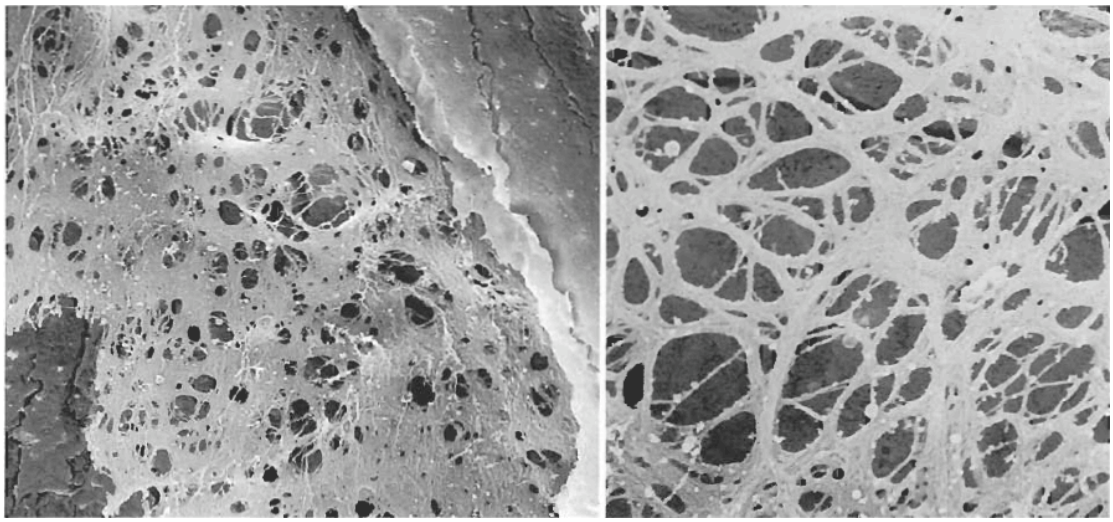

The collagen SEM image [43]

(a)

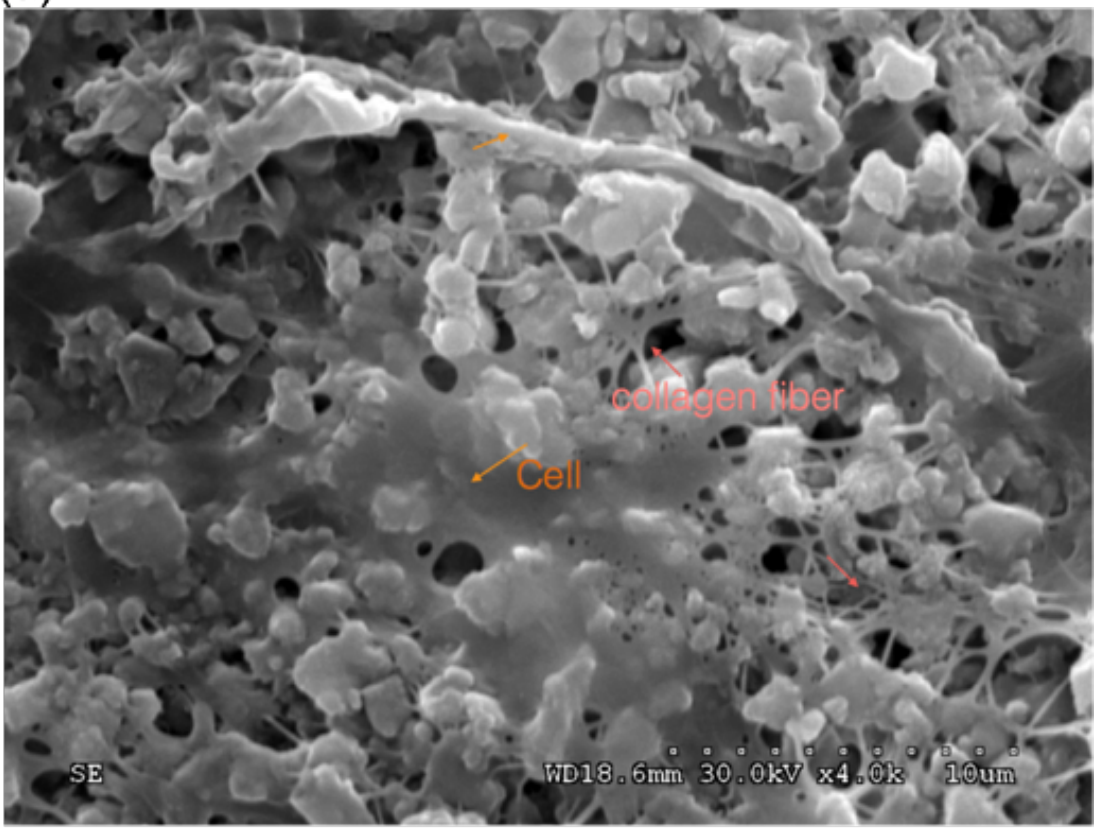
collagen fiber
Cell
SE
WD18.6mm 30.0kV x4.0k 10um

(b)

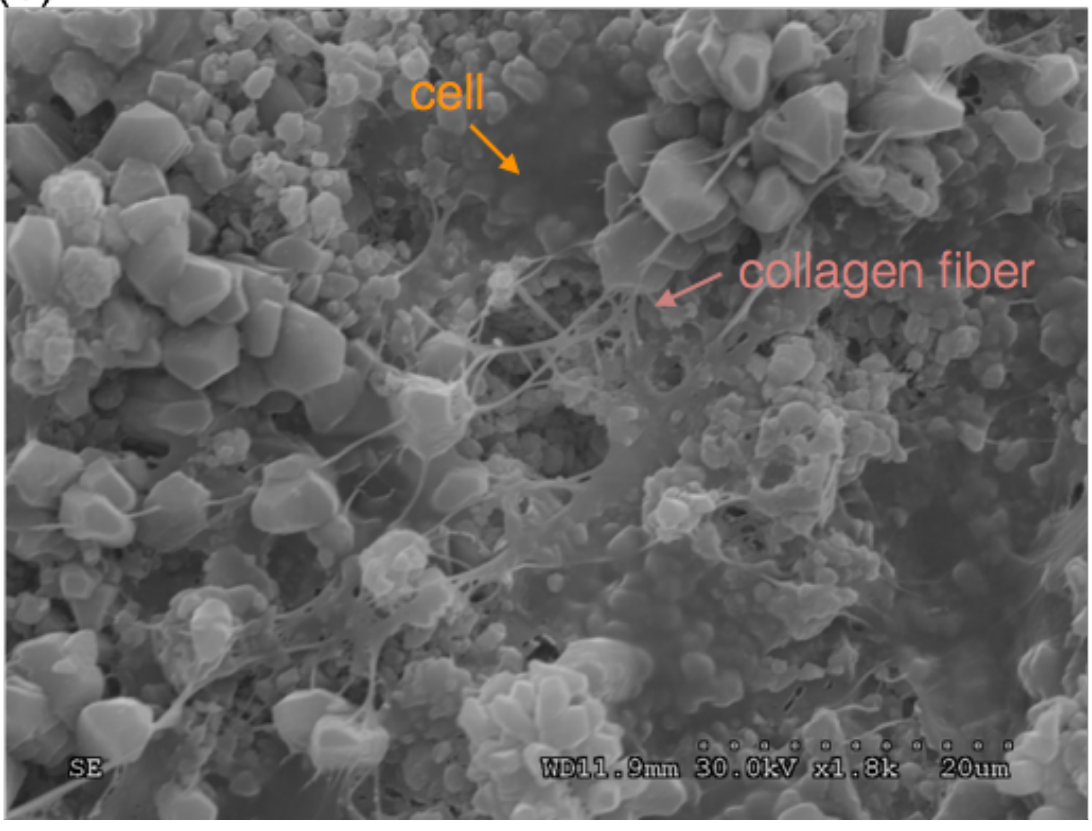
cell
collagen fiber
SE
WD11.9mm 30.0kV x1.8k 20um

Fig 4.21 The MC3T3 cells and the collagen fiber on the surface of 30%G--30%Bioglass/70% β-TCP with 2wt% Gelatin solution scaffold. The picture was taken after (a)21 days (b)28 days the cell seeded and Hitachi S-3000N Variable SEM in 30kV.

(a)

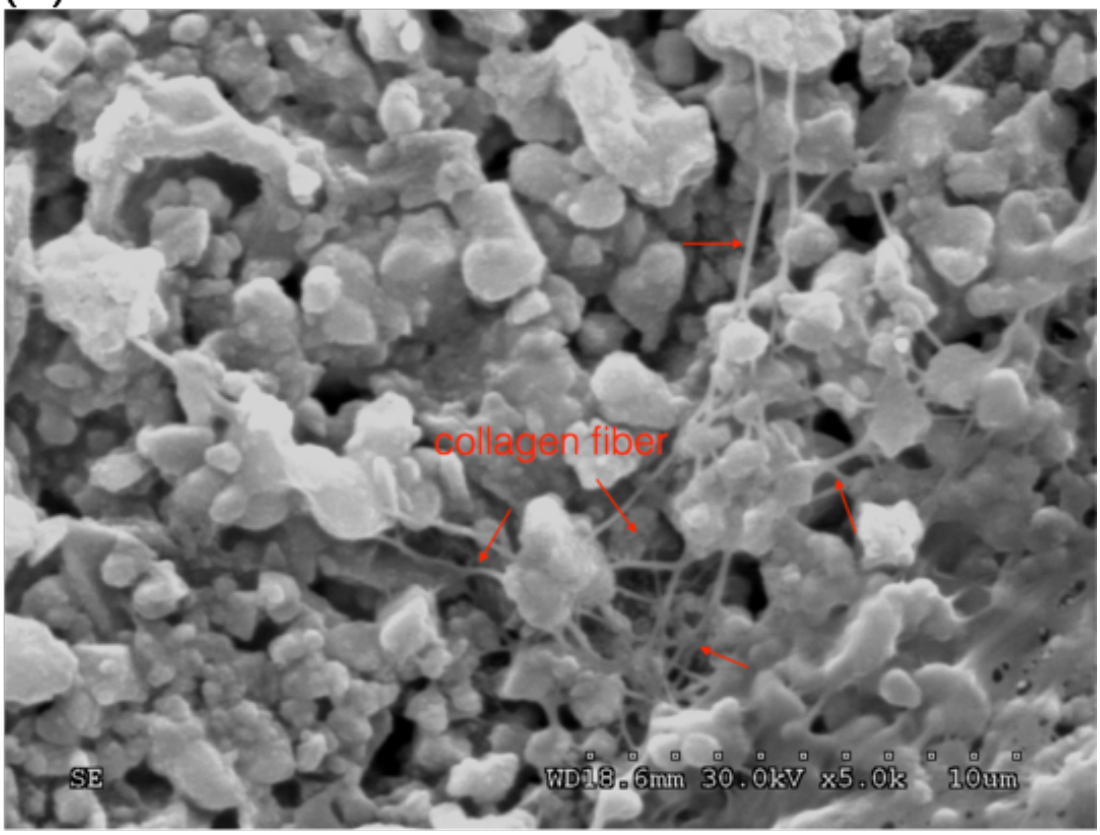
collagen fiber
SE
WD18.6mm 30.0kV x5.0k 10um

(b)

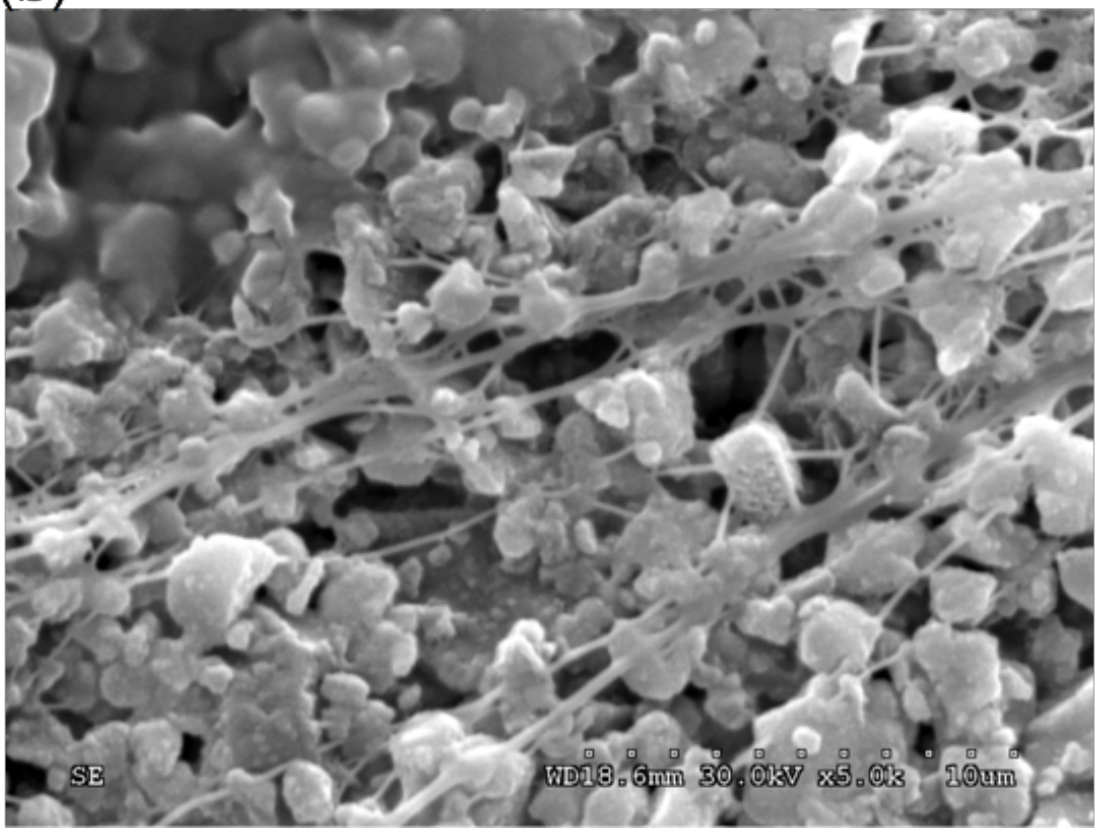
SE
WD18.6mm 30.0kV x5.0k 10um

Fig 4.22 Scanning electron microscopic observation of collagen fibril-bundles. The picture was taken after 21 days the cell seeded and Hitachi S-3000N Variable SEM in 30kV. (a) 30%L-- 30%Bioglass/70% β-TCP with 2wt% laponite solution scaffold 21 day (b) 30%--30%Bioglass/70% β-TCP with 2wt% Na_2HPO_4 solution scaffold for 21 day

4.4 Discussion

Injectability is expressed as the percentage of paste that can be extruded from a syringe, ideally in a homogeneous way under an applied force. The eventual occurrence of solid/liquid segregation (also known as filter pressing effect) during injection worsens or even hinders injectability. This study demonstrated a quality assessment rather than a quantity result since variety of factor influence the results. For more precise result, some study showed that to use the testing machine to measure to performed the experiment under certain circumstance[39][31]. The loads and displacement were fixed and the machine will stop as no more displacement can be put on the cement. In this case, the result will be more quantized and reliable.

Calcium phosphate biocements still encounter a situation by a dissolution–precipitation reaction which the cement continuously dissolves to form a supersaturated solution and will precipitate from the aqueous cement phase and forms a complicated crystal matrix. The mechanical strength of a cement matrix will result in crystal entanglement and the porosity of the final product determine the final porosity. Literature shows that porosity reduction in cements from 50% to 31% if compression can increase by nearly an order of magnitude.[52] Though porosity reduction by decreasing the amount of cement liquid used for mixing, the liquid still act as a good factor for in vitro study, like gelatin. Study show that a compensation way to maintain the mechanical property and the cytocompatibility by coating on the surface of scaffold. Some researches have demonstrated that the surface coating of substrates with gelatin enhances the attachment and proliferation of cells.[42] With a method of dispersed the β-TCP bioglass composite scaffold to a higher concentration (3 wt.%) gelatin solution was further mixed for 15 second by the homogenizer. The surface of scaffold will be homogenous covered by gelatin coating. This process can lead to no matter higher mechanical property and the bioactive property. β-TCP which has been extensively explored as one osteogenic substrate, was combined. β-TCP

incorporation enabled the gelatin sponge to increase the compression modulus without any change in the pore structure.[55]

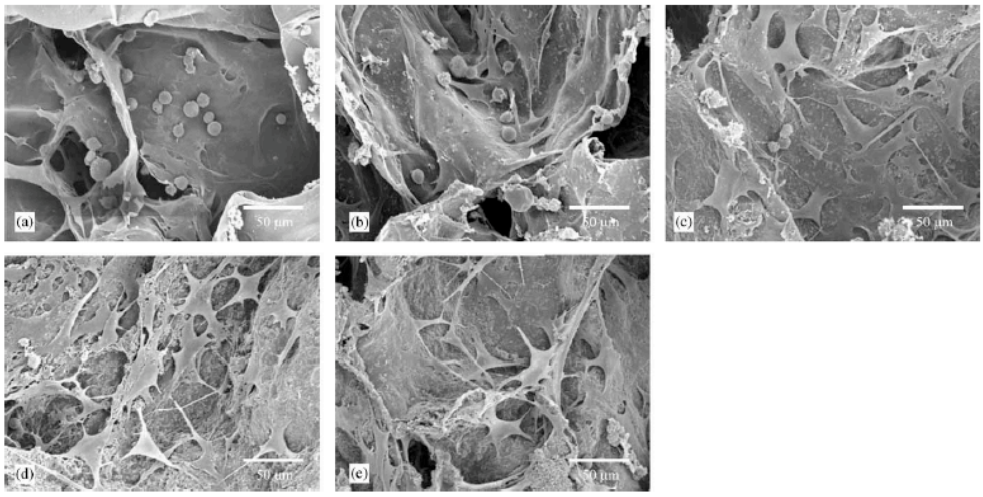

Fig 4.23 Scanning electron micrographs of MSC attached to gelatin sponges incorporating. [56]

The product of the setting reaction is quite often calcium deficient hydroxyapatite (CDHA), which exhibits structural and chemical properties similar to biological apatite. A variety of different compositions have been proposed for CPCs leading to CDHA in hydrolysis process. As a matter of fact, the properties of a cement, such as setting time and final strength, can be modulated through variation in powder composition, liquid phase, powder-to-liquid ratio[57]. At a temperature of about 40°C, gelatin aqueous solutions are in the sol state and undergo gelification when they are cooled at room temperature. Thus, the addition of gelatin to the CPCs

is expected to improve the workability and the mechanical properties of the cement. The composite cement powder (about 18wt% gelatin, and 82wt% a-tricalcium phosphate) and 5wt% of $CaHPO_4 \cdot 2H2O$ were added to the powder before mixing with the liquid phase. By elevating the total volume of gelatin can still lead to the fewer setting time (2 day after soaking in SBF) of CDHA formation and the 5wt% of $CaHPO_4$ also can help to increase the mechanical property from 10.7 to 14.0MPa[55].

4.5 Conclusion

Beta tri-calcium phosphate (β-TCP) combined with materials like gelatin and laponite become several kinds of β-TCP bioglass composite and has also overcome the drawback of its poor material properties. It forms CDHA from day one in the result of FTIR and form a lot after 7 day setting observed by the XRD pattern Especially the 30%BG +70% β-TCP/ Gelatin and 30%BG+ 70%β-TCP/ laponite groups prove the **4 times faster of the HA formation** then the 20% BG+ 80% β-TCP groups. About the mechanical property, all the groups can be compatible to pig trabecular bone at day 28 especially the *30%BG+70% β-TCP bioglass gelatin composite* reached **1.36 times** to the real bone. About the most well known draw back

of β-TCP, the injectability, *30%BG+70% β-TCP bioglass gelatin cement* almost can be extruded all up to 95% of injectability.

Undoubtedly, it is successful help tissue regeneration to make use of cells constituting tissue to be regenerated and differentiated in the viability and proliferation study. Bone is a natural composite of collagen protein and the mineral hydroxyapatite. During the formation of bone, collagen molecules assemble into fibrils. In the vitro study also observed that the β-TCP bioglass composite can lead to in vitro osteogenic differentiation of MC3T3-El subclone 4 and forming collagen fiber. Mineralized collagen protein matrix can form Collagen–HAP composites. It is not only the basic building blocks of the human bone, but they are also amongst the most abundant class of bio mineralized materials.

With some finding of the material property and biological property, the final aim of printing a porous scaffold was ready to move to the 3D printing part.

Chapter 5

Three Dimensional Printed Scaffold

5.1 Introduction

A lot of interest has been put into the utilization of bioactive ceramic materials in the repairing and regeneration of bone defects[58]. The driving force for calcium phosphate-based bioactive ceramic development is because of its well-established osteoconductive properties and the defected bone available for placement in or around defects. This autografts is good for reconstructing small bone defects and have strong osteogenic characteristics relevant to bone healing, modeling, and remodeling.[59] In recent years, tissue engineering has developed as an alternative strategy for bone grafts.[60] This method relies on the use of combinations of specific cell types, growth factors and three dimensional (3D) porous scaffolds

This chapter is for creating the simple 3D structures for in vitro composite tissue mimicking the three-dimension structure of bone and discuss a setting environment when it applied to 3D printing machine when it applied to extrude process.

Growth and differentiation of osteoblasts are often studied in cell cultures. however, osteoblasts are embedded within a complex three-dimensional (3D) micro environment, which bears little relation to standard culture flasks. Our study characterizes osteoblast-like cells cultured in 3D bioactive scaffold. Primary rat osteoblasts and MC3T3-E1 cells were seeded to the porous scaffolds to observe the cell adhesion phenomenon.

β-TCP has been widely used as bone scaffold material due to good bioactivity, and biocompatibility. However, the poor mechanical properties such as compressive strength and fracture toughness have severely restricted its use to low load-bearing applications, but with the intrinsic and extrinsic design they can achieve higher mechanical properties. When it comes to a porous scaffold, sometimes the mechanical property will decrease since the gap between individual filaments cannot endure more applied force due to porosity considerably lowers the strength and stiffness (Young's

modulus) of the cements matrix with an inverse exponential relationship between cement porosity and compressive strength[61]

$$CS = CS_0 exp^{\sim 2Kp} (1)$$

(1) where CS is the compressive strength at a given porosity; CS_0 is the maximum theoretical strength of the material; K is a constant; and P is porosity

Therefore, it is relevant to improve the strength and toughness, and further improve the bioactivity. Generally, it has been believed that liquid phase sintering is an effective way to improve the mechanical properties of ceramics[62]. So the sintered process will also be introduced in this chapter.

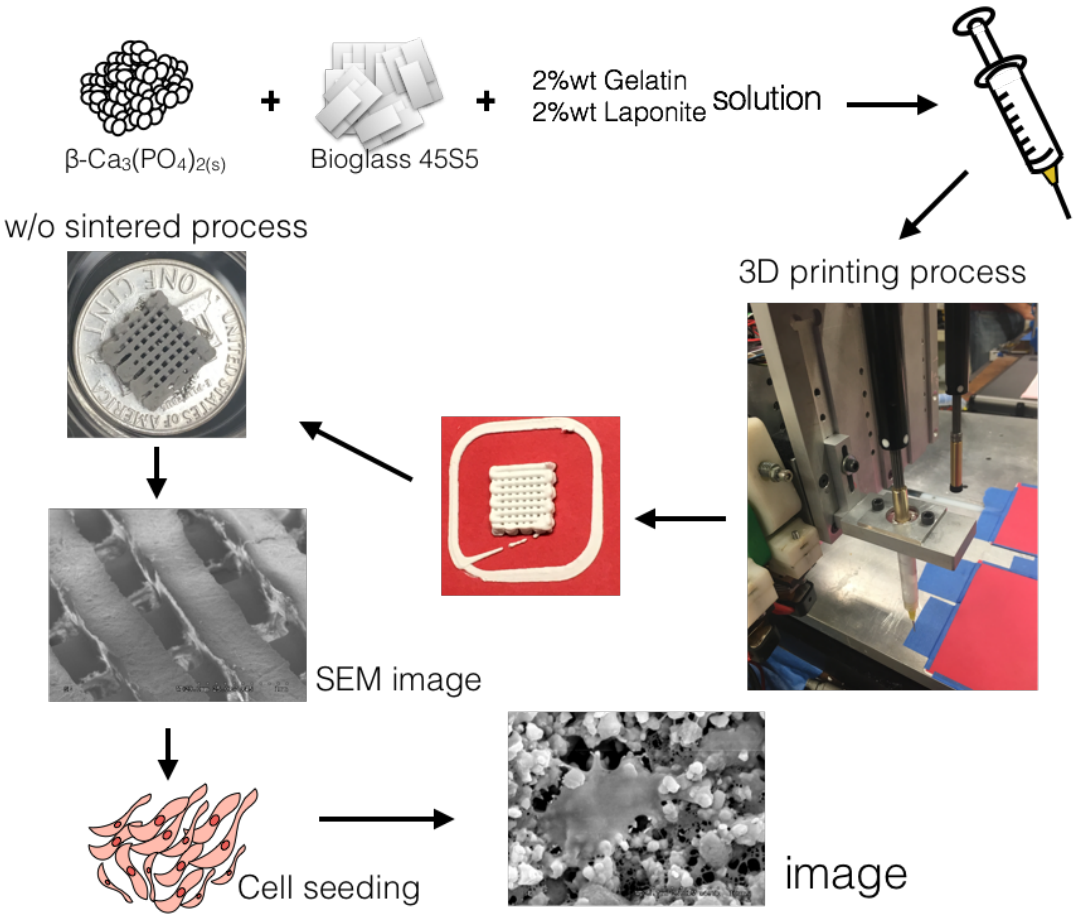

Fig 5.1 The experiment procedure for three dimensional printing task/ experiment method.

5.2 Materials and Methods

5.2.1 Material preparation

The cement mixture was prepared by ball milling β –TCP and bioglass 4S5S (BG) by the proportion of 7:3(30%BG) and mixing with, 2wt% gelatin and 2wt%

laponite solution. Setting experiments of the liquid phase were also prepared by using deionized water. Samples were prepared by mixing the powder with the required liquid volume with P/L=1/0.5 with a mortar and pestle for 2-3 minutes, and packing the cement into a standard 3ml syringe with 9mm inner diameter, 65mm length, and 0.65mm needle diameter with length ~13mm (Kahnetics Dispensing Tips).

5.2.2 3D printer description

X-Y-Z motion platform from Microkinetics with 0.003mm motion resolution was modified in-house into an additive manufacturing environment at the MARS Laboratory under the supervision of Dr. Panos Shiakolas in the Department of Mechanical & Aerospace Engineering at the University of Texas at Arlington. A double-stacked NEMA 11 linear actuator from (Haydon Kerk) was utilized for the syringe-based printing of the prepared bioceramic mixture. The machine was controlled using softwares Slic3r and Repetier-Host to generate motion commands for the layer-by-layer fabrication of the porous scaffolds. The scaffold CAD model was designed using SolidWorks software. The print speed utilized was 10mm/sec for all the scaffolds.

5.2.3 Sintering Process

The three dimensional scaffold was put in room temperature for dry out and then put on a Al_2O_3 alumina ceramic plate into a furnace to sintered up to 700°C for 1 h with Thermolyne 6000 Muffle Furnace. After the sintered process, the sample were cooling down for another day then prepared for analysis.

5.3 Porous Structure

The pattern of the porous scaffold was designed using a CAD model with 10mm x 10mm x 3mm square pattern with 6 layers. At first, the machine would extrude a bigger outline for continuing flow and eliminate of air blocked void of the cement and start to print after the steady of flow. The cement would be print on different direction of pattern and layers. The nozzle-bed distance was ~0.5mm.

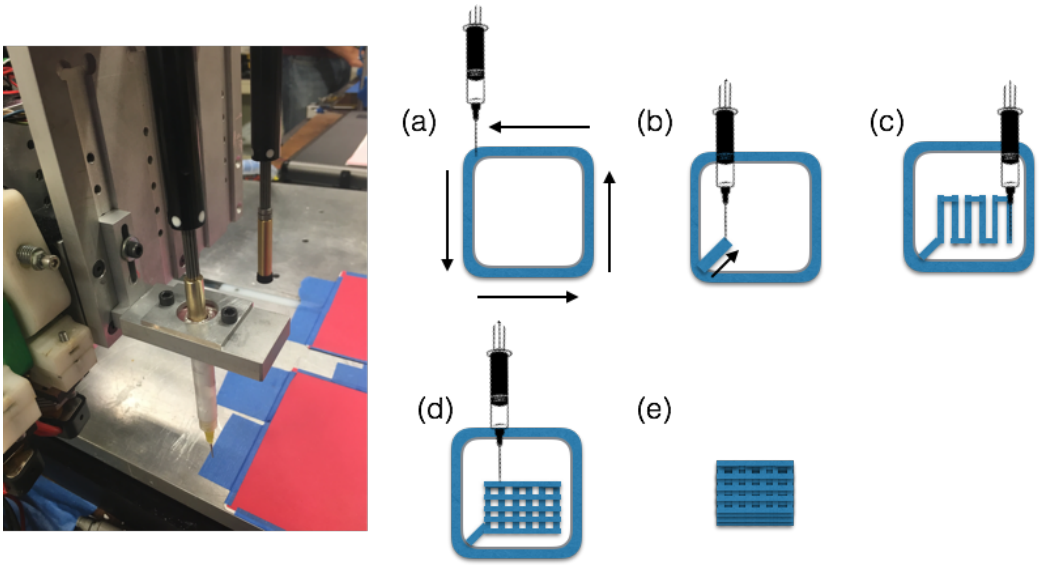

Fig 5.2 The walking step of printing a porous 3D scaffold.

5.4 Results and Discussion

5.4.1 Image/ SEM image

The sample were printed with three dimensional printers and then dry out for one day. After selected (sintered/ non sintered) sputtering with silver on the top of the bioactive porous scaffold. Image was taken by by Hitachi S-3000N Variable SEM. The gap size of the scaffold. The pore size of scaffold with the proportion of 7:3(30%BG) and mixing with 2wt% laponite solution without sintering was 524 ± 44.77 μm and line thick was around 620 μm in fig 5.3; The pore size with same proportion but with sintering was 441 ± 48.8 μm and 700-720 thick of the line in fig5.4. The pore would reduce 15.8% on estimated and the line will increase around 16%. More detail of the sintered would be considered as the “melting” phenomenon of our grain particle size and lead to the compensation of the pore reduced and line

expanded in Fig 5.5. The fig5.6 shows the cross section of 3D scaffold by SEM microscopy.

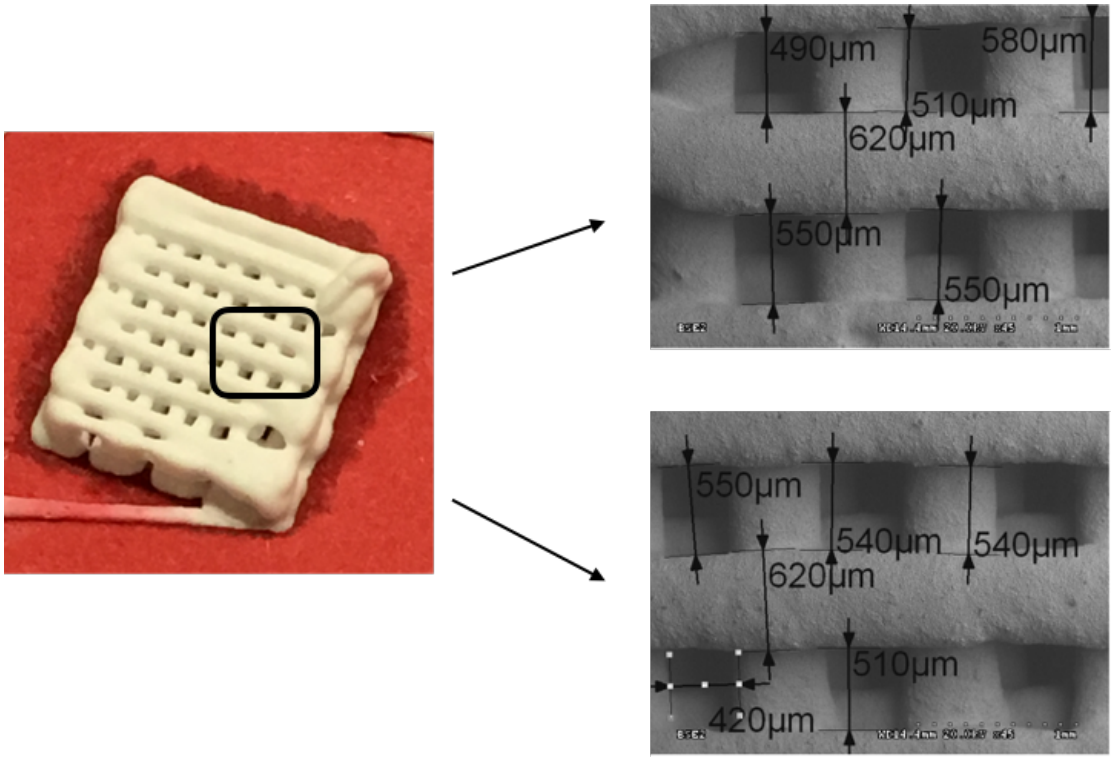

Fig 5.3 The pore size of 7:3(30%BG) and mixing with 2wt% laponite solution without sintering was 524 ± 44.77 µm, and the line thick was around 620 µm

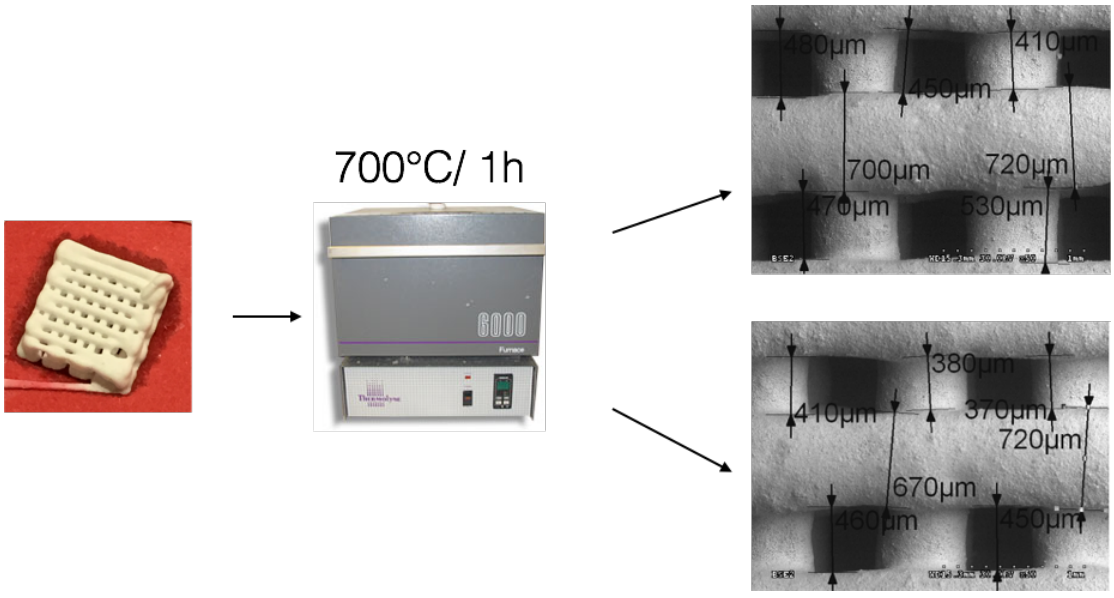

Fig 5.4 The pore size of 7:3(30%BG) and mixing with 2wt% laponite solution with sintering at 700℃/ 1h was 544 ± 48.8 μm and 700-720 thick of the line. The pore would reduce 15.8% on estimated and the line will increase around 16%. The pore and line make a compensation of each other.

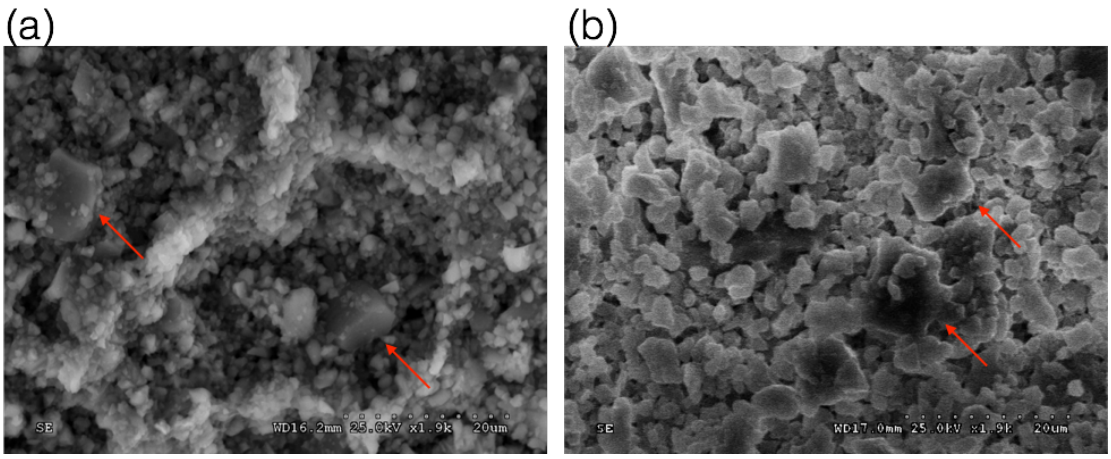

Fig 5.5 The melting phenomenon of Bioglass 45S5 when sintered up to 700℃ for 1 hour (a) 30%BG/Na2HPO4 non-sintered (b) 30%BG/Na2HPO4 sintered at 700℃ for 1 hour

Fig 5.6 The cross-section area of porous scaffold

5.4.2 Sintered process

The development of bioactive glass-ceramic materials has been a topic of great interest aiming at enhancing the mechanical strength of traditional bioactive scaffolds. On the other hand, melting of the crystalline phases present in the starting glass-ceramic material at elevated temperatures may result in the total densification of the porous structure. The XRD pattern indicated that when sintered at 630 ℃ may be assigned to partial crystallization of the bioglass and formation of a glass ceramic with characteristic peaks for sodium calcium silicates. The XRD pattern indicated that

the exothermal peak at 630 ℃ may be assigned to partial crystallization of the bioglass and formation of a glass ceramic with characteristic peaks for sodium calcium silicates.[25] When bioactive glass 45S5 heating up to 700℃, the amorphous phase will become crystalline in fig 5.7. We can also find the increasing peak intensity around 34° which is the most significant peak from crystalline Bioglass and the peak was more obviously in 30% BG Group in fig 5.8

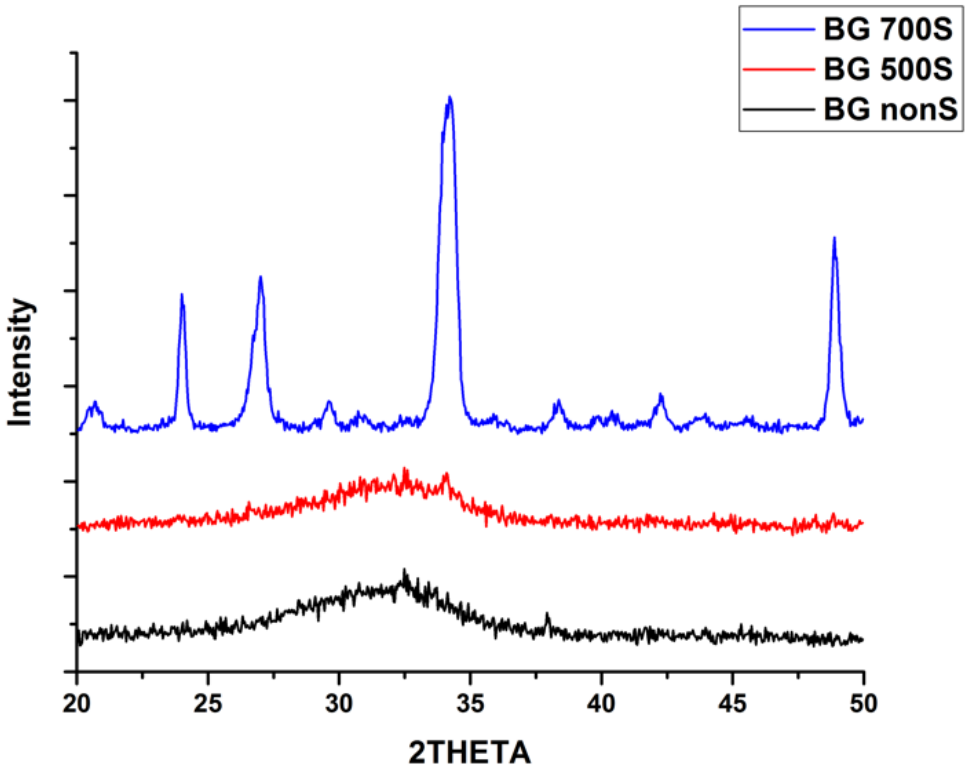

Fig 5.7 X-ray diffraction pattern of Bioglass 45S5 sintered at different temperature. The crystalline phase will form when heating above 700℃.

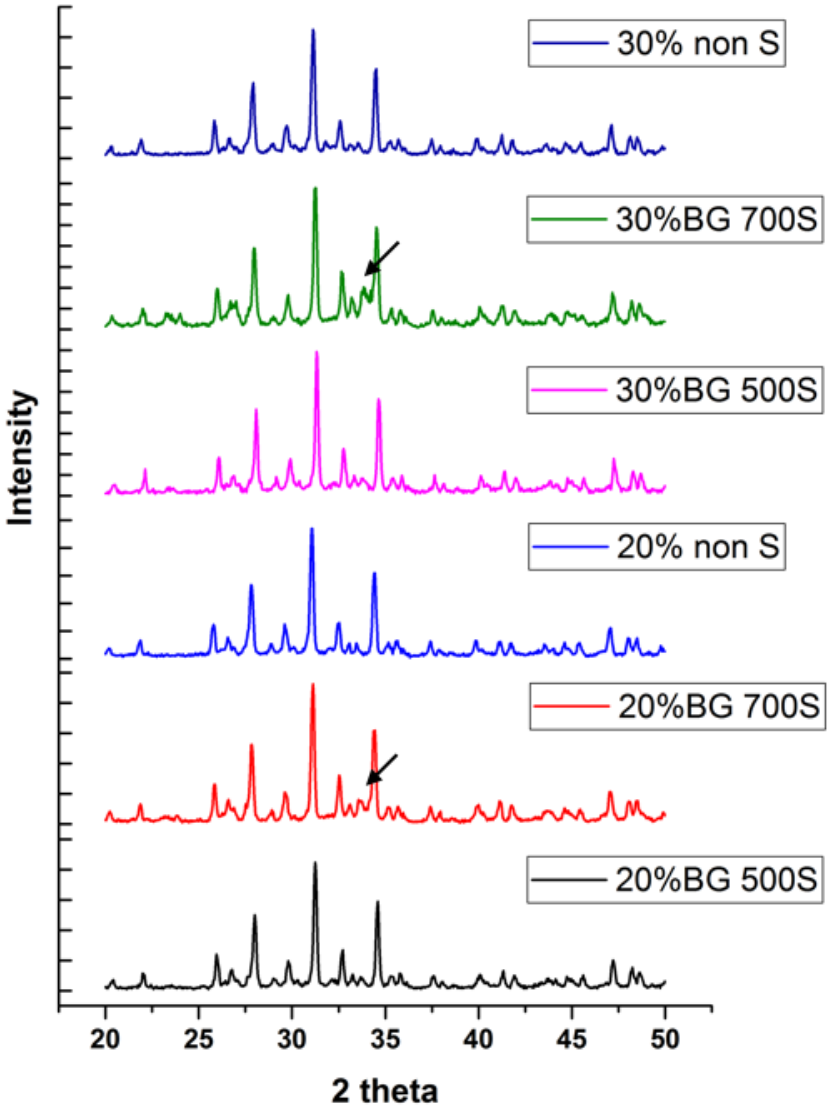

Fig 5.8 The x-Ray pattern with sintered and non sintered groups "→" means eaks for sodium calcium silicates. From up to down 30%bioglass and 70% β-TCP with 2wt%Na_2HPO_4 solution sintered at non-sintered/700℃/500℃ and 20%bioglass and 80% β-TCP with 2wt%Na_2HPO_4 sintered at non-sintered/700℃/500℃

5.4.3 EDS mapping

Surface morphology, scaffold composition, and element distribution were investigated using scanning electron microscopy (Hitachi S-3000N Variable Pressure SEM) equipped with an energy dispersive X-ray spectrometry system (EDAX). SEM images were taken with an acceleration voltage of 20.0 kV and scans for EDX mapping and compositional studies. EDAX software was used to quantify spectral mapping data from vision areas. Four regions of interest (ROIs) corresponding to Si, O, N, and P Kα lines were defined. The 30% Bioglass and 70% β-TCP with 2wt% laponite solution sample (30% laponite) non-sintered and sintered at 700℃ were analysis for element distribution in fig 5.9 and 5.10. We can identify that the Si line was more obvious after sintered and some crystallization happened.

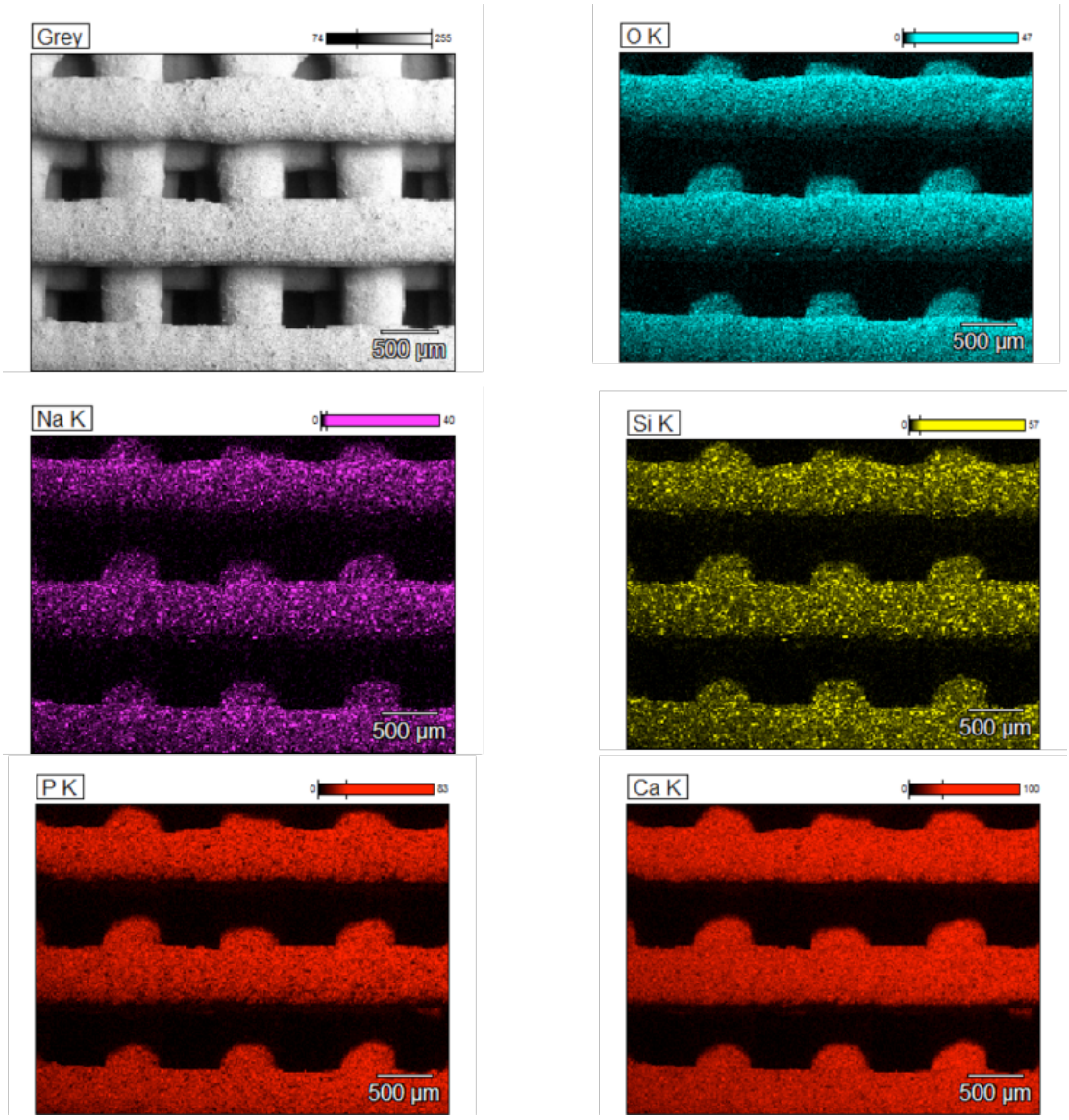

Fig 5.9 EDS mapping of 30% laponite non-sintered.

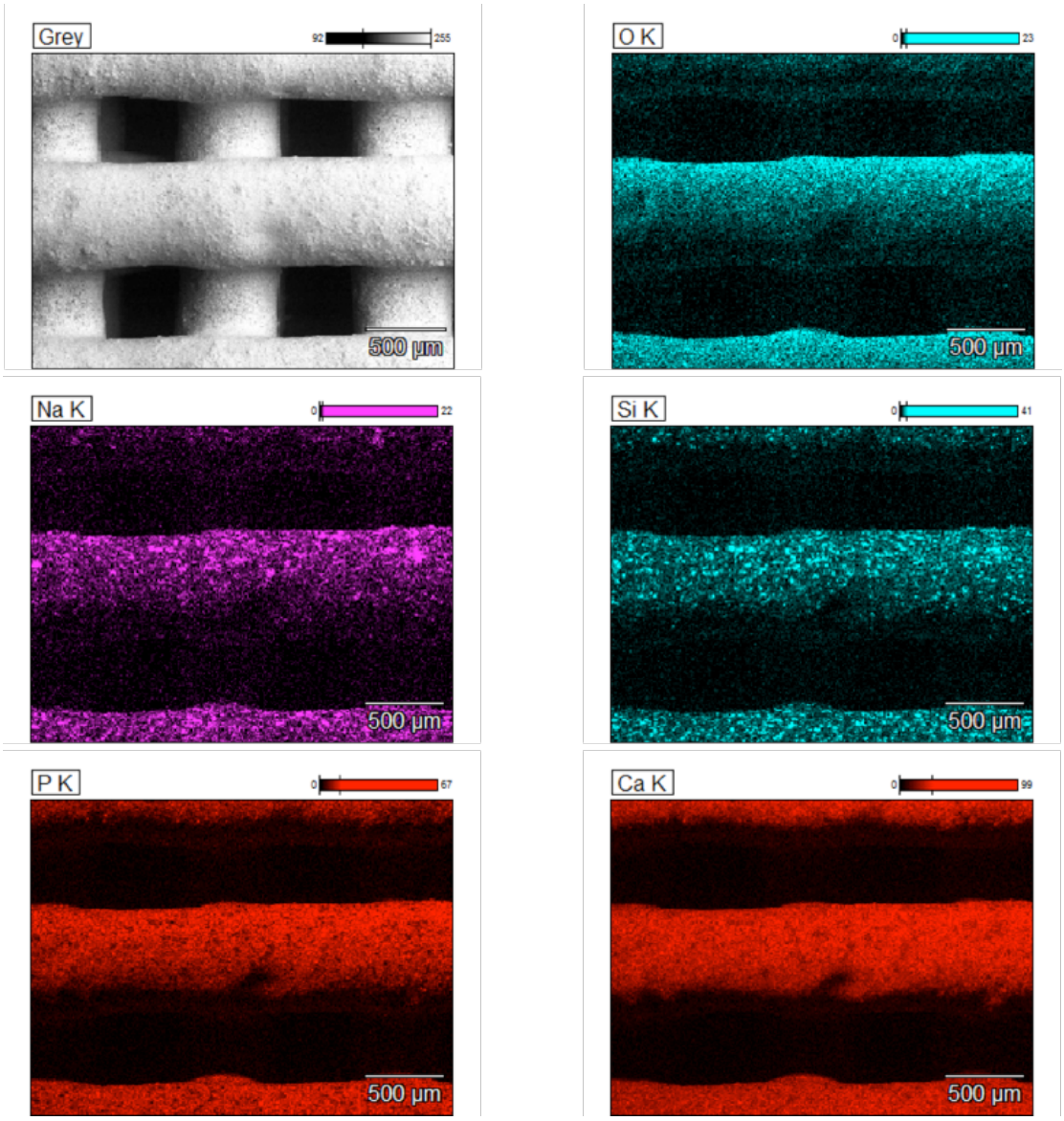

5.10 EDS mapping of 30% laponite sintered at 700℃ for one hour. More obvious of Si line showed on mapping elements distribution.

5.4.4 Cell attachment

The optimal scaffold for bone repair should be closely fit the damaged bone area, prevent infection, provide mechanical stability, recruit cells to the site for repair, promote fast bone growth into the scaffold, and eventually remodel leaving normal bone behind. Using this three-dimensional (3D) printing porous scaffold, we can design custom scaffolds with different pattern for bone repair composed of materials with these optimal characteristics and combine them with some coatings or growth factor that can provide improved healing. The cell of of MC3T3-El subclone 4 cell was seeded on the 3D scaffold in fig 5.11

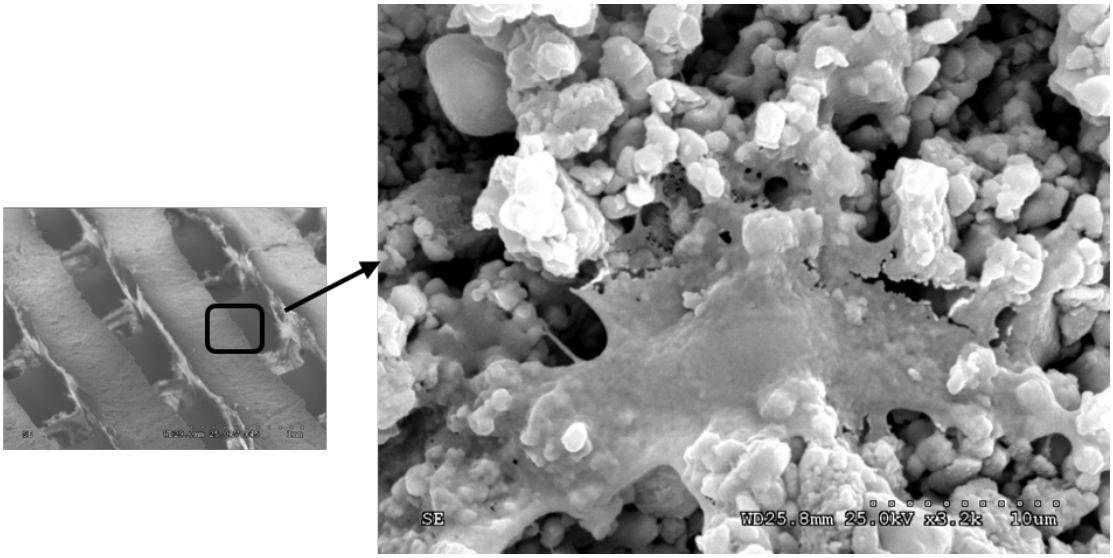

Fig 5.11 The SEM image of MC3T3-El subclone 4 cell on porous bioactive scaffold for 3 days.

5.5 Conclusion

The development and the usage of three dimensional (3D) printed porous scaffolds represents an opportunity for the regenerative medicine field. However, once a design is created and fabricated, evaluation of what is a successful design for host integration remains a non-standardized process. This application of 3D printing process combined set of methods, the setting, that can be used to identify scaffold designs for enhanced the efficiency to print out a scaffold continuously and stably.

This chapter consists of the following techniques: (i) The material setting, (ii) the machine and software basic setting, (iii) biocompatibility testing, and (iv) scaffold molding. (v) the sintered process. These methods evaluate scaffolds by identifying the possibility of printing and designing for the 3D scaffolds.

With the knowledge of injectability testing, we can apply that to the printing process. With modified β-TCP cement, the structure can be created and remain to a stable process of printing under the setting of the machine's step and force applied. A porous can not only help to create a custom design of implant scaffold and also mimic the real environment of pathology and also allow the researcher to understand the impacts

of small changes in pore size, sintered process which may impact cell and tissue in growth.

Chapter 6

Application

Bioceramics have been considered for use as synthetic bone graft substitutes (BGSs) for over 30 years. This modified β-TCP bioglass composite scaffold can be applied in two types of application(i) The cement type (ii) The 3D structure scaffold

6.1 The cement type of biomaterial

The cement type injectable substitute can reduce the number of surgical procedures and provide some function like (a) The void can be filled with a biocements and can therefore not be invaded by fibrous tissue; (b) β-TCP bioglass composite cement hardens in situ, augments the bone, and provides some mechanical stability; (c) β-TCP bioglass composite cement acts as a scaffold for the ingrowth of bone. The injectability is also enhanced and make flow easily and the injection may be performed without high pressure. When bone-forming cells are in direct contact with the β-TCP bioglass cement (or may be concrete after setting time), the

hydroxyapatite particles get incorporated into the newly formed bone which increases the bone strength. In a fracture or a bone defect, bone cell proliferation initiates cartilage growth followed by immature bone formation. If the mechanical situation is stable, woven and lamellar bone will follow. To activate healing in a void not created by surgery or a recent fracture, it is preferable to provoke bleeding to attract cells and to promote angiogenesis and subsequent bone healing.

Fig 6.1 Bioactive cement can help to fill in the void when fracture happened and promote the bone healing.[63]

The different kind of biomaterial can be applied to kinds of bone failure. The 3D structure can be printed into a fracture or a crack, completely dissolves over time, while in its place the human body regenerates the missing part of the bone tissue. This can be applied to more serious bone failure and can create a certain shape of scaffold that fit the failure area. Compare to the 3D scaffold, the biocements can treat the situation that is more slightly symptom like some crack of fracture of bone. In this case, the biocements can just inject and fill into the fracture void and no need for surgery. With evaluation, this two kinds of material can be applied to different kinds of bone failure

6.2 The 3D structure scaffold

The field of tissue engineering is actively investigating tissue-replacement solutions, many of which involve 3D scaffolds. Scaffolds must provide a balance of shape, biomechanical function and biocompatibility in order to achieve tissue replacement success. Customized 3D scaffold can obtain the goal of creating an optimal shape that can fit in different region of bone fracture. Different tissues can have different requirements for success, which has led to the development of various materials with unique characteristics. With different geometry of patter can create a variety of scaffold the meet the expectation of different region bone failure.

Fig6.2 3D scaffold can be applied to different region of bone defect and fit the injury part (Meets Downloadable Designs: 3D Printing from CAD to Metal)

Appendix A

Solid state reaction of β-TCP synthesis

1. Mix $CaHPO_4$(Monetite) and $CaCO_3$ in a 2:1 molar ratio. Ca/P ratio 1.50.

2.CaHPO4(s)+ CaCO3(s) -> β-Ca3(PO4)2(s)+ CO2(g)+ H2O(g)

CaHPO4 MW=136.06g/mol; CaCO3 MW=100.09g/mol; β-Ca3(PO4)2 MW=310.18g/mol

Example:

0.1mole β-Ca3(PO4)2= 31.018g product

needs 0.2mole CaHPO4(s)=27.212g

0.1mole CaCO3 =10g

3. Ball mill for 24h in a 250 ml polyethylene bottle with zirconia balls of 10mm and 2mm (Ratio between zirconia balls weight and powder weight is 6.21), and Keep wet environment with ethanol (99.9%) 1ml per 1g of powder

Example:

0.1mole β-Ca3(PO4)2= 31.018g product

reactant powder is 37.212g needs 231g zirconia balls

ethanol= 37ml

4. After ball milling the mixture will be dried in an oven at 60℃ for ethanol and crush it then use ethanol to moisturize to fill it in the mold.

5. Put them in the ceramic container (4-6 sample per container), heating them in furnace for 1050℃ for 24hr (low limit: 1050℃ high limit:1100℃ dwell time/remaining time:1440mins)

6. Crush the sample with mortar and pestle (sample pretty hard!! Be careful)

7. Ball milling the powder for 12hr to have fine powder

REFERENCES

[1] M. R. Brinker and D. P. O'Connor, "The Incidence of Fractures and Dislocations Referred for Orthopaedic Services in a Capitated Population," *J. Bone Jt. Surg.*, vol. 86, no. 2, pp. 290–297, Feb. 2004.

[2] M. Bohner, "Calcium orthophosphates in medicine : from ceramics to calcium phosphate cements," 2000.

[3] C. Du, F. Z. Cui, X. D. Zhu, and K. De Groot, "Three-dimensional nano-HAp / collagen matrix loading with osteogenic cells in organ culture," 1998.

[4] C. T. Laurencin, M. A. Attawia, L. Q. Lu, M. D. Borden, H. H. Lu, W. J. Gorum, and J. R. Lieberman, "Poly (lactide-co-glycolide)/ hydroxyapatite delivery of BMP-2-producing cells : a regional gene therapy approach to bone regeneration," vol. 22, pp. 1271–1277, 2001.

[5] A. A. Ignatius, M. Ohnmacht, L. E. Claes, J. Kreidler, and F. Palm, "A Composite Polymer / Tricalcium Phosphate Membrane for Guided Bone Regeneration in Maxillofacial Surgery," pp. 564–569, 2001.

[6] J. C. yuji Yin, Fen ye, “preparation and characterization of macroporous chitsan/gelatin beta tri calcium phosphate composite scaffold,” 2003.

[7] A. Félix, E. De Almeida, E. Cristina, and A. Ortega, “Applied Surface Science Synthesis of chitosan / hydroxyapatite membranes coated with hydroxycarbonate apatite for guided tissue regeneration purposes,” vol. 257, pp. 3888–3892, 2011.

[8] R. G. Carrodeguas and S. De Aza, “Acta Biomaterialia a -Tricalcium phosphate : Synthesis , properties and biomedical applications,” vol. 7, pp. 3536–3546, 2011.

[9] J. M. Oliveira, R. N. Correia, and M. H. Fernandes, “Surface modifications of a glass and a glass-ceramic of the - system in a simulated body fluid,” vol. 16, no. 11, pp. 649–654, 1995.

[10] H. Gray, C. M. Goss, and S. P. T. Mitchell, “Anatomy of the human body,” p. 1466, 1973.

[11] T. L. C. and S. K. Douglas J. DiGirolamo, “The skeleton as an endocrine organ.” 2012.

[12] T. A. G. and L. K. M. Katherine N. Weilaecher, “Cancer to bone: afatal attraction.” 2011.

[13] M. M. Stevens, “Biomaterials for bone Materials that enhance bone regeneration have a wealth of potential,” vol. 11, no. 5, pp. 18–25, 2008.

[14] J. C. Le Huec, T. Schaeverbeke, A. Le Rebeller, D. Clement, and J. Faber, “Influence of porosity on the mechanical resistance of hydroxyapatite ceramics under compressive stress,” vol. 16, no. 2, pp. 113–118, 1995.

[15] L. Liang, P. Rulis, and W. Y. Ching, “Acta Biomaterialia Mechanical properties , electronic structure and bonding of a - and b -tricalcium phosphates with surface characterization,” vol. 6, pp. 3763–3771, 2010.

[16] R. M. O. Hara, J. F. Orr, F. J. Buchanan, R. K. Wilcox, D. C. Barton, and N. J. Dunne, “Acta Biomaterialia Development of a bovine collagen – apatitic calcium phosphate cement for potential fracture treatment through vertebroplasty,” vol. 8, pp. 4043–4052, 2012.

[17] J. G. and U. G. Martha Geffers, “Reinforcement Strategies for Load-Bearing Calcium Phosphate Biocements,” 2015.

[18] B. J. Wang, C. Liu, Y. Liu, and S. Zhang, “Double-Network Interpenetrating Bone Cement via in situ Hybridization Protocol,” pp. 3997–4011, 2010.

[19] C. R. E. F. Id and C. Library, “Rapid #: -10729202,” 2016.

[20] R. T. U. Gburecka,*, O. Grolmsa, J.E. Barraletb, L.M. Groverb, “Mechanical Activation and Cement Formation of Beta-Tricalcium Phosphate,” vol. 9612, no. November, 2003.

[21] L. L. Hench, “Bioceramics : From Concept to Clinic.”

[22] S. K. Nandi, B. Kundu, and S. Datta, “Development and Applications of Varieties of Bioactive Glass Compositions in Dental Surgery , Third Generation Tissue Engineering , Orthopaedic Surgery and as Drug Delivery System,” 2003.

[23] M. MAGINOT, “CHEMICAL CHANGES IN DMP1-NULL MURINE BONE& SILICA BASED PECVD COATINGS FOR TITANIUM IMPLANTOSSEO APPLICATIONS,” no. August, 2014.

[24] O. P. Filho, G. P. Latorre, and L. L. Hench, “Effect of crystallization on apatite-layer formation of bioactive glass 45 %,” vol. 30, pp. 509–514, 1996.

[25] T. J. Brunner, R. N. Grass, and W. J. Stark, “Glass and bioglass nanopowders by flame synthesis {,” pp. 1384–1386, 2006.

[26] P. Hung, Y. Kuo, H. Chen, H. K. Chiang, and O. K. Lee, “Detection of Osteogenic Differentiation by Differential Mineralized Matrix Production in Mesenchymal Stromal Cells by Raman Spectroscopy,” vol. 8, no. 5, pp. 1–7, 2013.

[27] S. A. Redey, S. Razzouk, C. Rey, G. Leroy, M. Nardin, and G. Cournot, “Osteoclast adhesion and activity on synthetic hydroxyapatite , carbonated hydroxyapatite , and natural calcium carbonate : Relationship to surface energies,” 1998.

[28] B. Feng, J. Y. Chen, S. K. Qi, L. He, J. Z. Zhao, and X. D. Zhang, “Characterization of surface oxide ® lms on titanium and bioactivity,” vol. 3, pp. 457–464, 2002.

[29] M. Bohner and G. Baroud, “Injectability of calcium phosphate pastes,” vol. 26, pp. 1553–1563, 2005.

[30] S. V Dorozhkin, “Functional Biomaterials Self-Setting Calcium Orthophosphate Formulations,” pp. 209–311, 2013.

[31] M. Habib, G. Baroud, F. Gitzhofer, and M. Bohner, “Mechanisms underlying the limited injectability of hydraulic calcium phosphate paste,” vol. 4, pp. 1465–1471, 2008.

[32] B. M. Gumbiner, “Cell Adhesion : The Molecular Basis of Tissue Architecture and Morphogenesis,” vol. 84, pp. 345–357, 1996.

[33] M. W. Makgoba, A. Bernard, D. C. Road, C. De Service, D. Nice, and A. Pathways, “adhesion/signalling: biology and clinical applications,” 1992.

[34] K. Anselme, A. Ponche, and M. Bigerelle, “Relative influence of surface topography and surface chemistry on cell response to bone implant materials . Part 2 : biological aspects,” vol. 224, pp. 1487–1507, 2016.

[35] A. H. Reddi, R. Gayt, S. Gayt, and E. J. Millert, “Transitions in collagen types during matrix-induced cartilage , bone , and bone marrow formation,” vol. 74, no. 12, pp. 5589–5592, 1977.

[36] C. J. Doillon, M. G. Dunn, E. Bender, and F. H. Silver, “Collagen Fiber Formation in Repair Tissue : Development of Strength and Toughness,” vol. 5, pp. 481–492, 1985.

[37] R. Z. Legeros, “Calcium Phosphate-Based Osteoinductive Materials,” pp. 4742–4753, 2008.

[38] S. V Dorozhkin, “Biomaterials Bioceramics of calcium orthophosphates,” *Biomaterials*, vol. 31, no. 7, pp. 1465–1485, 2010.

[39] P. M. C. Torres, S. Gouveia, S. Olhero, A. Kaushal, and J. M. F. Ferreira, “Acta Biomaterialia Injectability of calcium phosphate pastes : Effects of particle size and state of aggregation of b -tricalcium phosphate powders,” vol. 21, pp. 204–216, 2015.

[40] M. Fathi, A. El Yacoubi, A. Massit, and B. C. El Idrissi, “Wet chemical method for preparing high purity β and α - tricalcium phosphate crystalline powders,” vol. 6, no. 6, pp. 139–143, 2015.

[41] S. V Dorozhkin and S. V Dorozhkin, “Calcium orthophosphates Calcium orthophosphates a n d e,” vol. 2535, no. June, 2016.

[42] E. F. Burguera, H. H. K. Xu, and L. Sun, “Injectable Calcium Phosphate Cement : Effects of Powder-to-Liquid Ratio and Needle Size,” pp. 493–502, 2007.

[43] Tatsuo Ushiki, “COLLAGEN FIBER, RETICULAR FIBER ANS ELASTIC FIBERS: A COMPREHENSIVE UNDERSTANDING FROM A MORPHOLOGICAL VIEW POINT.pdf.” 2002.

[44] S. V Dorozhkin and M. Epple, “Biological and Medical Significance of Calcium Phosphates.”

[45] P. Nevsten, L. Lidgren, and I. Mccarthy, “The Effect of Crystallinity on Strength Development of ⎵ -TCP Bone Substitutes,” pp. 159–165, 2006.

[46] S. Meejoo, W. Maneeprakorn, and P. Winotai, “Phase and thermal stability of nanocrystalline hydroxyapatite prepared via microwave heating,” vol. 447, pp. 115–120, 2006.

[47] G. Penel, C. Delfosse, M. Descamps, and G. Leroy, “Composition of bone and apatitic biomaterials as revealed by intravital Raman microspectroscopy,” vol. 36, pp. 893–901, 2005.

[48] H. J. Yvon, “Raman Bands RAMAN DATA AND ANALYSIS Raman Spectroscopy for Analysis and Monitoring,” pp. 2–3.

[49] M. M. J. Tecklenburg, “Carbonate Assignment and Calibration in the Raman Spectrum of Apatite,” pp. 46–52, 2007.

[50] G. S. Mandair and M. D. Morris, “Contributions of Raman spectroscopy to the understanding of bone strength,” *Bonekey Rep.*, vol. 4, no. August 2014, pp. 1–8, 2015.

[51] S. Bin Sulaiman, T. K. Keong, C. H. Cheng, A. Bin Saim, R. Bt, and H. Idrus, “Tricalcium phosphate / hydroxyapatite (TCP-HA) bone scaffold as potential candidate for the formation of tissue engineered bone,” no. June, pp. 1093–1101, 2013.

[52] M. Geffers, J. Groll, and U. Gbureck, “Reinforcement Strategies for Load-Bearing Calcium Phosphate Biocements,” 2016.

[53] L. Ghasemi-mobarakeh, M. P. Prabhakaran, and M. Morshed, “Author ’ s personal copy Biomaterials for nerve tissue engineering.”

[54] Z. Ma, C. Gao, Y. Gong, J. Ji, and J. Shen, “Immobilization of Natural Macromolecules on Poly-L-Lactic Acid Membrane Surface in Order to Improve Its Cytocompatibility,” no. January, pp. 838–847, 2002.

[55] A. Bigi, B. Bracci, and S. Panzavolta, “Effect of added gelatin on the properties of calcium phosphate cement,” vol. 25, pp. 2893–2899, 2004.

[56] Y. Takahashi, M. Yamamoto, and Y. T. Ã, “Osteogenic differentiation of mesenchymal stem cells in biodegradable sponges composed of gelatin and b - tricalcium phosphate,” vol. 26, pp. 3587–3596, 2005.

[57] F. C. M. Driessens, M. G. Boltong, E. A. P. D. E. Maeyer, and R. M. H. Verbeeck, “Effect of temperature and immersion on the setting of some calcium phosphate cements,” vol. 1, pp. 453–457, 2000.

[58] Victoria Galkowski; Petrisor Brad; Drew Brian;, “Bone stimulation for fracture healing: What’s all the fuss?,” p. 40399251, 2009.

[59] V. T. A. Abcdefg, D. J. P. Acde, A. P. Bcde, A. S. Bcdf, C. D. S. Abcdef, and P. M. Abcdefg, “xenograft , and synthetic grafts in a trabecular bone defect : An experimental study in rabbits,” vol. 16, no. 1, pp. 24–31, 2010.

[60] A. Wiskott and S. Scherrer, “A 3D printed TCP / HA structure as a new osteoconductive scaffold for vertical bone augmentation,” pp. 55–62, 2014.

[61] J. E. Barralet, T. Gaunt, A. J. Wright, I. R. Gibson, and J. C. Knowles, “Effect of Porosity Reduction by Compaction on Compressive Strength and Microstructure of Calcium Phosphate Cement,” pp. 1–9, 2001.

[62] D. Desimone, W. Li, J. A. Roether, D. W. Schubert, C. Murilo, A. C. M. Rodrigues, E. D. Zanotto, A. R. Boccaccini, D. Desimone, W. Li, J. A. Roether, D. W. Schubert, M. C. Crovace, A. C. M. Rodrigues, E. D. Zanotto, and A. R. Boccaccini, "Biosilicate – gelatine bone scaffolds by the foam replica technique : development and characterization," vol. 6996, no. June, 2016.

[63] B. Healing and T. Monograph, "CERAMENT TM| BONE VOID FILLER Bone Healing Technical Monograph."

BIOGRAPHICAL

Chien-Ning YAO was born in Keelung, Taiwan in 02.18.1991. Graduated in China Medical University in 2012 with a B.S in Biotechnology and Science in Taichung, Taiwan. She loves her family and country Taiwan, but she wants to study abroad, to discover the world.

She started her Master research at the University of Texas at Arlington in 2014 under the supervison of Dr. Pranesh Aswath. Her current research interests include bone remodeling phenomena, beta tri calcium phosphate material, bioactive glasses, 3D porous biomaterial.

She completed her thesis work in Material Science and Engineering in 2016